Marine Pollution Bulletin 212 (2025) 117460

Contents lists available at ScienceDirect

Marine Pollution Bulletin

journal homepage: www.elsevier.com/locate/marpolbul

Saltwater intrusion and land subsidence destroy northern Nile Delta archaeological sites: An assessment using hydrochemical indices, SAR satellite imagery, and analytic hierarchy process (AHP)

Mohammed Hagage [a,*], Abdel Galil A. Hewaidy [b], Abdulaziz M. Abdulaziz [c]

[a] Engineering Applications and Water Division, National Authority for Remote Sensing and Space Sciences (NARSS), 23 Joseph Tito Street, El-Nozha El-Gedida, P.O. Box: 1564, Cairo, Egypt
[b] Geology Department, Faculty of Science, Al-Azhar University, El Nasr Street, P.O. Box 11751, Nasr City, Cairo, Egypt
[c] Faculty of Engineering, Cairo University, 1 Gamaa Street, P.O. Box 12613, Giza, Egypt

ARTICLE INFO

Keywords:
Archaeological risk map
Archaeological sites deterioration
Archaeological preservation
Climate change
Coastal archaeology
Groundwater salinization
InSAR
MCDA
Seawater intrusion
Water corrosion indices

ABSTRACT

Archaeological sites in deltaic regions face increasing environmental threats. This study provides the first assessment of seawater intrusion and land subsidence impacts on archaeological sites in the Nile Delta through hydrochemical investigations, InSAR techniques, and multi-criteria decision analysis of 33 sites. The results reveal that 80.7 % of groundwater samples are of the seawater (Na—Cl) type, with northern groundwater primarily consisting of old marine water. The Groundwater Quality Index for Seawater Intrusion shows that 54.6 % of sites have saline groundwater and 45.4 % have mixed groundwater. Hydrochemical Facies Evolution analysis indicates that 73 % of sites are north of the freshwater-seawater interface, with water tables <1 m deep. All sites show high risks of limescale accumulation and corrosive conditions. SBAS-InSAR analysis (2020–2024) detected displacement velocities between −16 and + 5 mm/year, with maximum subsidence in the northern region. The archaeological risk map was developed using the AHP, integrating water corrosion indices, water table depth, soil texture, and subsidence rates. The map classified the archaeological sites into four risk categories: 8 sites were classified as severe risk, 12 sites as high risk, 11 sites as moderate risk, and 2 sites as low risk. These findings highlight the urgent need for mitigation strategies, including groundwater level reduction and prioritized documentation of high-risk archaeological sites.

1. Introduction

Groundwater salinization caused by saltwater intrusion into freshwater aquifers represents a significant threat to the sustainability of coastal groundwater resources globally (Prusty and Farooq, 2020; Abd-Elaty et al., 2021; Chala et al., 2022; Perumal et al., 2024). This issue has become increasingly critical in recent decades due to the accelerating impacts of climate change, land subsidence, and excessive groundwater extraction. These factors have heightened the vulnerability of coastal regions and led to more frequent and severe instances of seawater intrusion (Costall et al., 2020; Taha et al., 2023; Puigserver et al., 2024).

Saltwater intrusion presents numerous environmental challenges, including salinization of freshwater resources and degradation of soil quality (Lü et al., 2023; Abd El-Hamid et al., 2023). These risks often coincide with dense archaeological heritage, as past civilizations frequently centered along fertile and navigable deltaic coastlines (Lecher and Watson, 2021; Hagage et al., 2023a; Howland and Thompson, 2024).

Land subsidence, the gradual sinking or settling of the ground surface, can result from various natural and anthropogenic factors (Deng et al., 2022). While natural processes like tectonic movements and sediment compaction contribute to subsidence, human activities often greatly exacerbate it, particularly through excessive extraction of groundwater, oil, or gas (Zhang et al., 2015; Othman and Abdelmohsen, 2022). The removal of subsurface fluids causes pore collapse and compaction, triggering subsidence of the overlying land (Gambolati and Teatini, 2015). This subsidence-induced deformation alters coastal zone topography, creating lower elevation relative to sea level and increasing vulnerability to seawater intrusion (Daito and Galloway, 2015; Prusty and Farooq, 2020; Chala et al., 2022).

* Corresponding author.
E-mail address: mohammed.hagage@narss.sci.eg (M. Hagage).

https://doi.org/10.1016/j.marpolbul.2024.117460
Received 22 September 2024; Received in revised form 12 December 2024; Accepted 12 December 2024
Available online 26 December 2024

Understanding the complex dynamics of seawater intrusion and land subsidence is imperative for sustainable management and planning endeavors (Gimenez-Forcada, 2019; Jasechko et al., 2020). Investigating the causes, rates, and spatial patterns of these phenomena provides valuable insights for developing effective mitigation and adaptation strategies (Abd-Elaty et al., 2021; Hajji et al., 2022). This necessitates integrating multidisciplinary approaches, including geological and geophysical surveys, hydrochemical investigation, remote sensing and GIS, numerical modeling, and socio-economic assessments to comprehend community impacts (Attwa et al., 2016; Hussain et al., 2019; Chala et al., 2022; Dieu et al., 2022; Abdelfattah et al., 2023).

Radar satellite imagery has revolutionized hydrogeological studies by allowing researchers to monitor extensive areas with high spatial resolution under various climate conditions (Musa et al., 2015; Mtibaa and Asano, 2022). Continuous monitoring of land subsidence through radar imaging provides crucial information for investigating seawater intrusion in coastal regions. This technology aids in identifying vulnerable areas, evaluating the effectiveness of mitigation measures, and guiding future management strategies (Costall et al., 2020; Bokhari et al., 2023). Synthetic Aperture Radar (SAR) satellite data has proven effective in measuring land subsidence resulting from aquifer overexploitation (Raspini et al., 2022; Reshi et al., 2023). Additionally, it facilitates the analysis of subsidence in regions affected by high tides, which can lead to seawater intrusion, coastal erosion, and groundwater depletion (Hakim et al., 2020; Bai et al., 2023).

Hydrochemical investigation is crucial for studying groundwater contamination by saltwater and evaluating potential damage to different surfaces (Baskaran et al., 2022; Ghosh and Jha, 2023; Shah et al., 2023). Hydrochemical indicators and diagrams provide direct evidence of saltwater intrusion and changes in groundwater quality while facilitating the visualization and interpretation of complex water chemistry data (Elbeih et al., 2021; Hussien et al., 2021; Hagage et al., 2022; Sangadi et al., 2022; Yu et al., 2023; Moorthy et al., 2024). Additionally, these investigations offer insights into the potential impacts of saline groundwater on archaeological materials (Hagage et al., 2023b; Shah et al., 2023), including risks such as chemical etching, pitting, salt weathering, scale buildup, and degradation when groundwater interacts with different surfaces (Kalyani et al., 2017; Kadam et al., 2021).

Additionally, the Analytic Hierarchy Process (AHP) is a robust multicriteria decision-making tool that has gained significant traction in environmental management (Echogdali et al., 2022; Elbeih et al., 2023; Singh et al., 2023). By breaking down complex problems into smaller, manageable components, AHP allows for systematic comparisons among various criteria, thereby enhancing the decision-making process (Sutadian et al., 2017). AHP has been instrumental in water management (Echogdali et al., 2022; Singh et al., 2023; Ozegin et al., 2024) and assessing threats to cultural heritage sites (Yagoub et al., 2023; Dammag et al., 2024).

The Nile Delta region, with its coastline along the Mediterranean Sea, exemplifies the challenges posed by saltwater intrusion and land subsidence. This area is home to a rich archaeological heritage, featuring numerous sites that contain artifacts and structures providing valuable insights into human history (Hendrickx and Claes, 2017; Zaghloul and E. A., 2019; Meister et al., 2021; Hagage et al., 2023a). Hagage et al. (2023a) utilized satellite imagery to examine landscape evolution in the northeastern Nile Delta, revealing multiple threats to archaeological tells, including rising groundwater levels and encroachment from agriculture and urban development.

Saltwater intrusion introduces chloride, sodium, and sulfate ions into groundwater, rendering it more corrosive and detrimental to archaeological sites (Hagage et al., 2023b; Howland and Thompson, 2024). This issue is magnified by the rising water table in the Nile Delta, permitting direct interactions between salt-enriched groundwater and archaeological materials, which accelerate degradation via chemical and physical weathering processes (Helmi and Hefni, 2016; Vallet et al., 2022; El-Hassan and Abd El-Tawab, 2023; Hagage et al., 2024).

Several studies have investigated saltwater intrusion into groundwater in the Nile Delta (e.g., Attwa et al., 2016; Abd-Elhamid, 2017; Mabrouk et al., 2018; Hussain et al., 2019; Abd-Elaty et al., 2021; Abd El-Hamid et al., 2023; Abdelfattah et al., 2023; Taha et al., 2023), attributing its worsening to a combination of natural factors and inadequate water management practices, including groundwater overextraction and rising sea levels. Additionally, multiple studies have utilized SAR images to assess land subsidence rates in the Nile Delta (Becker and Sultan, 2009; Aly et al., 2012; Gebremichael et al., 2018; Saleh and Becker, 2019; Rateb and Abotalib, 2020; Abou El-Magd et al., 2024). However, previous research has notable knowledge gaps:

1- Insufficient attention to the impacts of saltwater intrusion on archaeological sites and its consequences for archaeological materials and structures.
2- The interplay between land subsidence and saltwater intrusion, especially in relation to the deterioration of archaeological sites, remains unexamined.

To address these gaps, this study aims to:

1- Assess the severity of saltwater intrusion at archaeological sites and its implications for archaeological materials and structures. This will be achieved by employing hydrochemical saltwater intrusion indices and groundwater corrosion indices.
2- Calculate land subsidence using 93 Sentinel-1 SLC (Single Look Complex) scenes and investigate its implications for archaeological sites.
3- Develop an archaeological risk map using the Analytic Hierarchy Process (AHP). This will involve integrating various factors such as groundwater corrosion indices, water table depth, soil texture, and land subsidence data to assess potential risks to archaeological sites effectively.

The results of this research will offer valuable insights for water resource management and the preservation of cultural heritage in this historically and economically important region. Moreover, the findings can inform similar investigations in other coastal aquifers worldwide, contributing to global efforts to address the challenges posed by saltwater intrusion in the face of climate change.

2. Study area and problem definition

The study area is located in the northeastern Nile Delta, south of Lake Manzala (Fig. 1a). Spanning an area of 1047 km^2, it features a dense network of canals and drains, including the Bahr El-Baqar drain and El-Salam canal. The region experiences an arid climate with very low annual rainfall (20–100 mm/year), which significantly limits contributions to groundwater recharge (El-Sayed et al., 2018).

The primary groundwater storage unit consists of Early Pleistocene deposits (Quaternary aquifer), characterized by sand and gravel interspersed with clay lenses (El-Sayed et al., 2018). Overlying these deposits are Holocene sediments consisting of clay, Nile silt, and sandy clay, with thicknesses ranging from 10 to 30 m, functioning as an aquitard (Attwa et al., 2016). Surface water systems significantly influence groundwater dynamics, governing recharge rates, flow direction, water quality, and groundwater head (El-Aassar et al., 2023). Discharge occurs through pumping wells and seaward seepage into Lake Manzala (Abo-El-Fadl, 2013).

The study area includes 33 archaeological sites that span from the Prehistoric (5500–3100 BCE) to Byzantine (330–641 CE) periods (Fig. 1b, Supplementary Table 1). These sites are archaeological tells, shaped by millennia of continuous occupation. They comprise successive deposits both above and below ground level and contain artifacts and archaeological structures that provide valuable insights into the

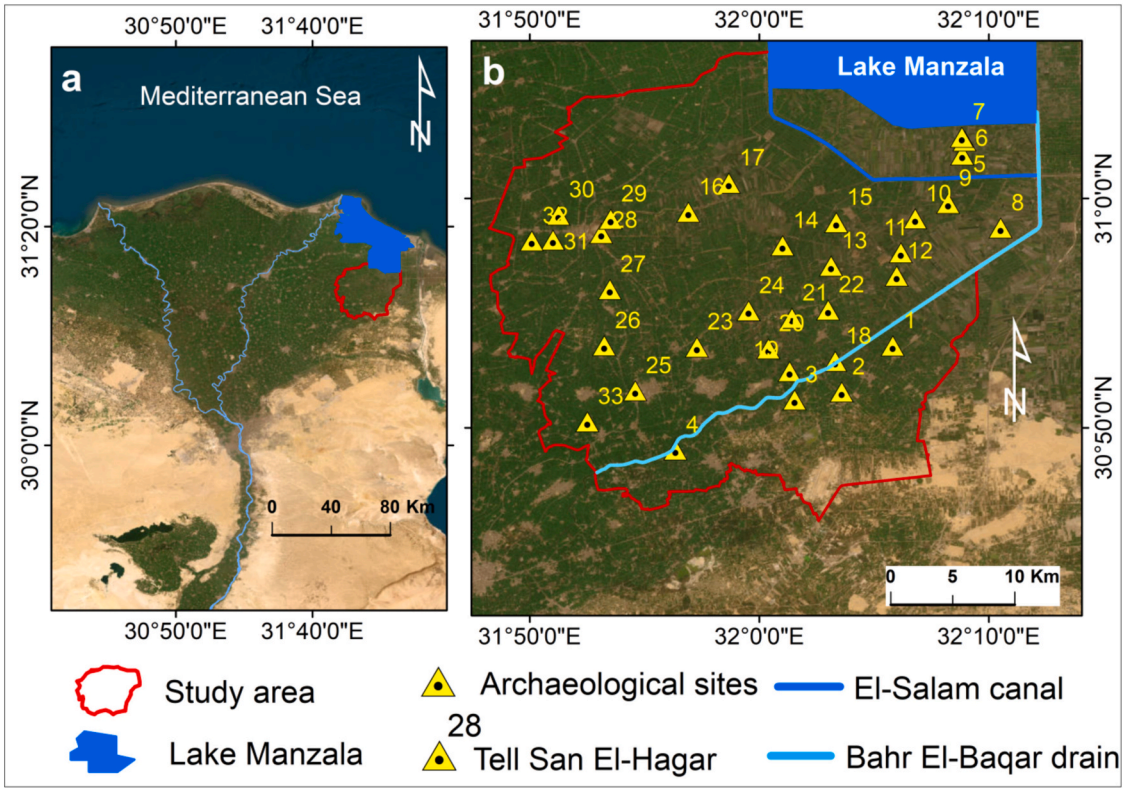

Fig. 1. Study area and archaeological site distribution in the northeastern Nile Delta. (a) Satellite image (Esri basemap) showing the location of the study area in the Nile Delta. (b) Spatial distribution of archaeological sites within the study area.

history and activities of the Nile Delta (Hagage et al., 2023a). The most renowned site is Tell San El-Hager (ancient Tanis), a residence and burial place for kings of the 21st-22nd Dynasty (1070–730 BCE), which includes an Amun temple and royal tombs (Helmi and Hefni, 2016; El-Hassan and Abd El-Tawab, 2023) (Fig. 2). Only the western area of Tell San El-Hager is being excavated, while excavation work has never begun on the rest of Tell San El-Hager and the other archaeological sites (Supp. Fig. 1a).

The water table in the region is situated near the Earth's surface, ranging from 0.6 to 3 m below ground level (Fig. 2a). This proximity places archaeological sites in direct contact with groundwater or within the zone of capillary rise, which exposes them to deterioration (Vallet et al., 2022; El-Hassan and Abd El-Tawab, 2023; Hagage et al., 2024). Furthermore, saltwater intrusion and land subsidence have been extensively observed in the Nile Delta (Rateb and Abotalib, 2020; Abd-Elaty et al., 2021; Taha et al., 2023; Abou El-Magd et al., 2024), potentially exacerbating deterioration issues (Supp. Fig. 1b,c). Moreover, the clay-dominated soil textures, coupled with the region's arid climate and high evaporation rates, further intensify salt accumulation (Arnous et al., 2015; Hammam and Mohamed, 2020).

The potential loss or deterioration of these archaeological sites would create an irreparable gap in our understanding of human history and the evolution of early urban centers worldwide. Given such challenges, there is an urgent need for a systematic assessment of the multiple hazards threatening archaeological sites in the northeastern Nile Delta. This study addresses these issues through a multi-methodological approach that combines hydrochemical analysis, advanced remote sensing techniques, and multi-criteria decision analysis. The resulting archaeological risk assessment will provide cultural heritage managers and policymakers with essential data for prioritizing conservation efforts and developing targeted mitigation strategies for the most threatened sites.

3. Methodology

This study employed a multi-faceted approach comprising four main components (Fig. 3): (1) field investigations, including groundwater and soil sampling, and in-situ measurements; (2) hydrochemical investigations; (3) remote sensing analysis using Interferometric Synthetic Aperture Radar (InSAR); and (4) geostatistical analysis and multi-criteria decision analysis utilizing the Analytic Hierarchy Process (AHP) to integrate deterioration factors, develop an archaeological risk map, and identify priority areas requiring urgent mitigation strategies.

3.1. Field sampling and analytical methods

Groundwater and soil samples were collected in April 2024, along with field measurements of water table depths across the study area. Thirty-four groundwater samples were obtained from wells tapping the shallow Quaternary aquifer, with depths ranging from 5 to 15 m below ground surface. Additionally, twenty-two soil samples were collected at depths of 100–120 cm to determine soil texture. All sampling locations were recorded using a Garmin GPS device and mapped using ArcGIS software version 10.7.1 (Fig. 4).

Standard methods (APHA, 2012) were followed for sample collection, preservation, and analysis. Rigorous quality assurance and quality control (QA/QC) protocols were implemented throughout the sampling, transportation, and laboratory analysis processes to ensure data accuracy and reliability. Field blanks and duplicates, comprising 10 % of the total samples, were collected to assess potential contamination during sampling and transportation and to evaluate analytical precision. Standard reference materials and calibration standards were utilized to validate laboratory instrument accuracy and procedural integrity.

Prior to groundwater sampling, wells were purged for several minutes to remove stagnant water. Field parameters (pH and electrical conductivity) were measured in situ using a Solinst interface meter.

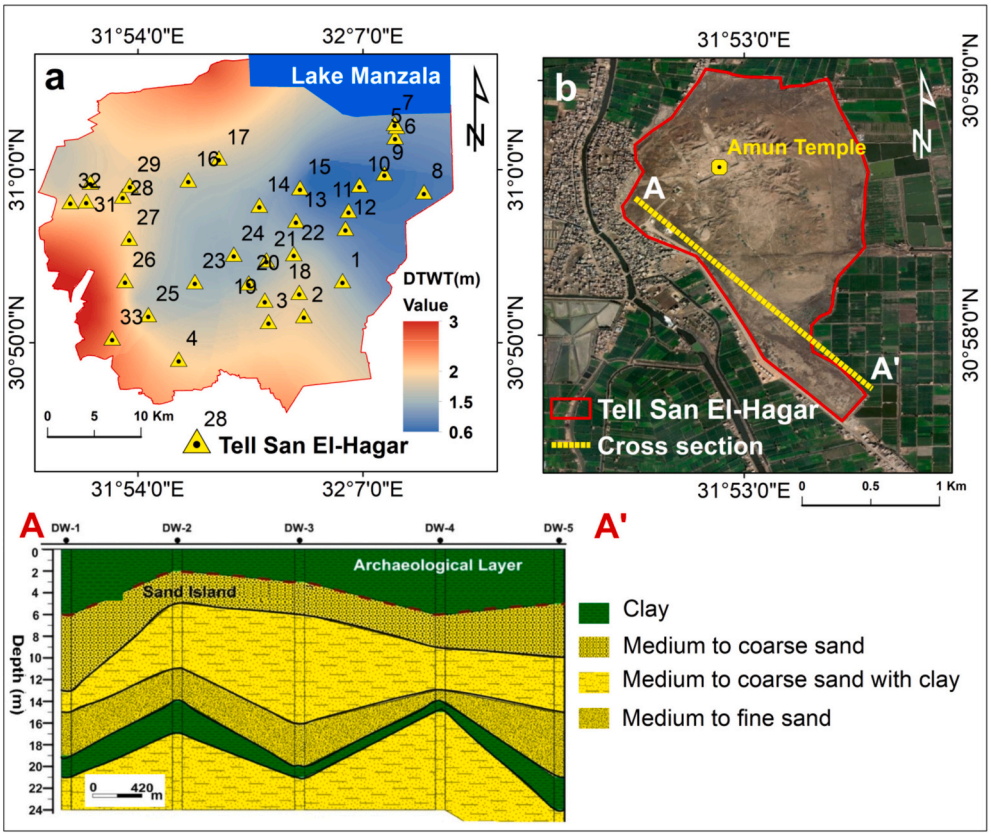

Fig. 2. (a) Depth to Water Table (DTWT) map illustrating the proximity of groundwater to the surface across the study region, based on a 2024 field survey. (b) Satellite image of Tell San El-Hagar (ancient Tanis) with an interpretive cross-section (adapted from Gaber et al., 2021), showing the archaeological clay layer containing artifacts extending to 6 m depth, demonstrating direct contact with the water table and vulnerability to capillary rise.

Water samples were filtered through 0.45 μm membrane filters, collected in polyethylene bottles, and stored on ice until analysis at the Central Laboratory for Environmental Quality Monitoring (CLEQM). Major cations and anions were determined using ion chromatography techniques (Srinivasan, 2017; Nesterenko, 2023).

Particle size distribution of soil samples was determined using the pipette method and used to classify soil texture according to the USDA soil texture triangle (Abdel-Fattah, 2019).

3.2. Hydrochemical indicators of saltwater intrusion

To effectively characterize and understand the dynamics of saltwater intrusion in the study area, a suite of hydrochemical indicators was employed. Three types of hydrochemical diagrams were utilized in this study to aid in interpreting water chemistry data and understanding its sources: the Chadha diagram, the Sulin diagram, and the hydrochemical facies evolution diagram (HFE—D). Microsoft Excel Worksheet and ArcGIS software version 10.7.1 were used to plot and calculate the data.

The Chadha diagram categorizes waters based on dominant ion types, which aids interpretation of prevailing hydrochemical processes affecting groundwater (Masoud et al., 2023; Rind et al., 2024). The Sulin diagram is used to determine groundwater types and origins by analyzing major ion ratios. It classifies groundwater genesis into four categories: old marine, recent marine, shallow meteoric, and deep meteoric (Megahed, 2020; Kumar et al., 2023).

The HFE diagram accounts for the dynamic nature of seawater intrusion by visualizing anion and cation percentages (Supp.Fig. 2a). It allows for better visualization of main hydrochemical processes and facies evolution during saltwater intrusion and freshening compared to diagrams like Piper (Giménez-Forcada et al., 2017; Dieu et al., 2022).

The HFE Diagram includes the Conservative Mixing Line (CML) separating freshwater from seawater (Supp. Fig. 2b). Groundwater samples located above the CML represent the freshening stage, while samples located below the CML represent the intrusion stage. Within the intrusion and freshening fields, sub-stages can be identified - freshening (f1-f4) and intrusion (i1-i4) (Gimenez-Forcada, 2019).

Additionally, the groundwater quality index for seawater intrusion (GQI_{SWI}) (Tomaszkiewicz et al., 2014) was calculated to evaluate saltwater intrusion in the shallow groundwater and its extent in archaeological sites. GQISWI combines typical water quality parameters signaling seawater intrusion into an understandable format to enable spatial analysis within a Geographic Information System (GIS) framework (Azari and Tabari, 2024). It combines the seawater fraction index (GQI_{fsea}) and the seawater-freshwater mixing index ($GQI_{Piper(mix)}$) based on Supp.eqs. 1 to 4 (Tomaszkiewicz et al., 2014). The GQI_{SWI} has proven effective for monitoring coastal aquifer saltwater intrusion in many regions (Baskaran et al., 2022; Ezzeldin, 2022; Hasan et al., 2023). It ranges from 0 to 100, where 0 indicates seawater and 100 is fresh water. Values above 75 represent freshwater, below 50 indicate saline/seawater, and 50–75 represent mixed-salinity groundwater (Rachid et al., 2015).

These methods have provided crucial insights into groundwater chemistry, origins, and the extent of saltwater influence, enabling a comprehensive assessment of saltwater intrusion at archaeological sites.

3.3. Groundwater corrosion and scaling indices

Two indices were used to evaluate the scaling and corrosion potential of groundwater on archaeological sites: the Ryznar Stability Index (RSI) and the Larson-Skold Index (LSI) (Supp.eqs. 5 and 6). The RSI measures the ability of water to dissolve or precipitate calcium carbonate ($CaCO_3$) (Islam, 2023). The RSI categorizes conditions into the

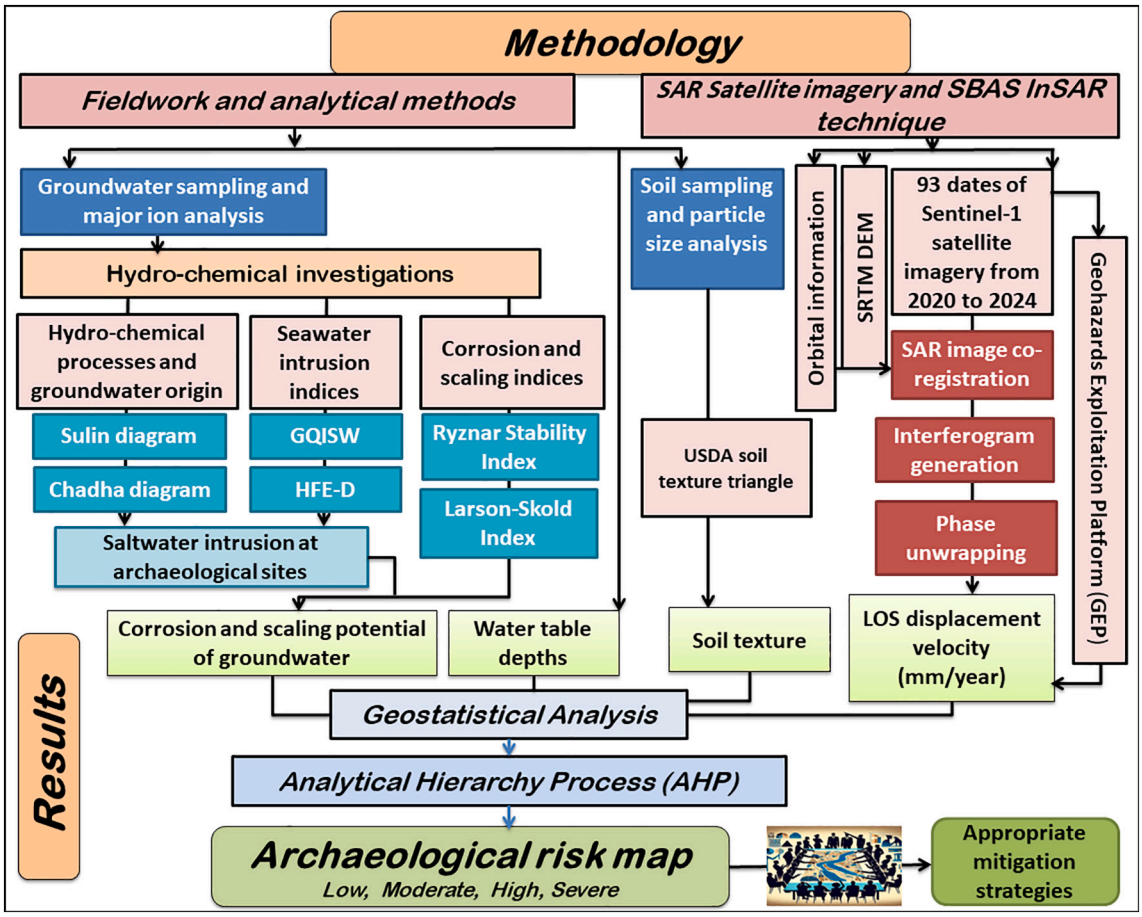

Fig. 3. Methodological framework flowchart illustrating the integrated approach for archaeological risk assessment.

following categories: heavy scaling (RSI values of 4–5), light scaling (RSI values of 5–6), little scaling or corrosion (RSI values of 6–7), significant corrosion (RSI values of 7–7.5), heavy corrosion (RSI values of 7.5–9), and intolerable corrosion (RSI values >9.0) (Ahmed et al., 2021). The RSI was chosen specifically because calcium carbonate is a major component of the archaeological building materials found in the study area (Gaber et al., 2021; El-Hassan and Abd El-Tawab, 2023).

Additionally, the LSI evaluates the overall degree of corrosiveness of groundwater relative to different surfaces by comparing the concentration of aggressive anions (chloride, sulfate) to passivating anions (bicarbonate, carbonate) (Kalyani et al., 2017). LSI values <0.8 indicate non-corrosive water, LSI values between 0.8 and 1.2 indicate significant corrosion potential, and LSI values >1.2 indicate high corrosion potential (Kadam et al., 2021). The LSI index was selected because it depends on the concentration of chloride and sulfate, which are ions characteristic of groundwater exposed to saltwater intrusion.

3.4. InSAR data acquisition and processing

Precise quantification of slow subsidence rates in the Nile Delta requires numerous SAR images over extended periods using InSAR techniques. This study utilized 93 Sentinel-1 SAR scenes acquired from 2020 to 2024 to assess land subsidence in the northeastern Nile Delta (Table 1).

The Sentinel-1 SAR scenes were acquired as Single Look Complex (SLC) products in Interferometric Wide Swath (IW) mode with VV polarization along ascending orbit track 58 from the ESA repository. The IW TOPSAR scans cover a 250 km swath width at 5 × 20 m pixel resolution (ESA, 2023). Due to the unavailability of complementary Sentinel-1B coverage over the study region after 2021, only Sentinel-1A data with its 12-day revisit cycle was used.

The Parallel Small Baseline Subset (P-SBAS) approach was employed to process the Sentinel-1 SAR scenes using the "CNR-IREA P-SBAS Sentinel-1 on-demand" service on the ESA Geohazard Thematic Exploitation Platform (https://geohazards-tep.eu). The SBAS algorithm is a widely applied multi-temporal DInSAR technique that generates ground deformation time-series by analyzing interferogram stacks with small spatial and temporal baselines to maximize coherence (De Luca et al., 2015). P-SBAS, a recent advancement of the SBAS algorithm, is designed for rapid generation of deformation time series. It utilizes distributed computing systems, including High-Performance Computing (HPC) and Cloud Computing environments, leveraging multiple processors for more efficient processing (Foumelis et al., 2022). The approach has demonstrated effectiveness in processing large Sentinel-1 IW datasets, providing valuable insights into ground deformation (De Luca et al., 2018; Manunta et al., 2019; Abou El-Magd et al., 2024).

The P-SBAS workflow incorporated several key inputs: Sentinel-1 SLC data, precise orbital data, and a digital elevation model (DEM). A 30 m Shuttle Radar Topography Mission (SRTM) DEM from NASA was used for co-registration and topographic phase removal. The main outputs were line-of-sight (LOS) displacement velocity, used to characterize land subsidence across the study area (Supp. Fig. 3).

3.5. Analytical hierarchy process (AHP) and archaeological risk map

The development of the archaeological risk map integrated four main criteria: scaling and corrosion indices (RSI & LI), water table depth (WTD), soil texture (ST), and land subsidence (LS). The methodology followed these steps:

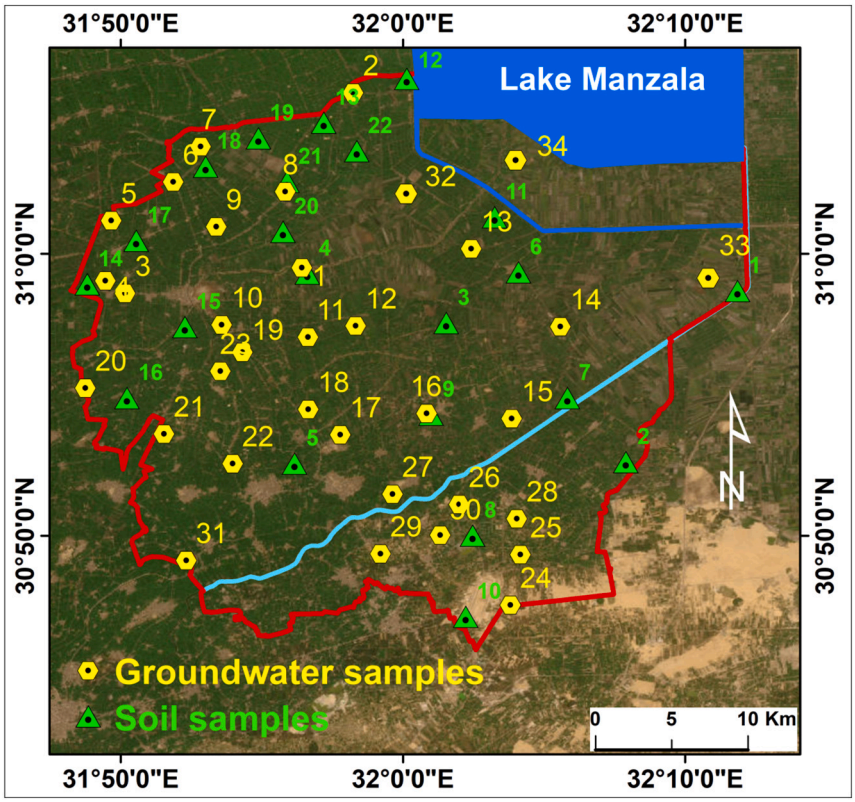

Fig. 4. Map showing locations of collected groundwater and soil samples created using ArcGIS software version 10.7.1 [https://desktop.arcgis.com].

Table 1
Key characteristics of the SAR data and processing parameters used in the study.

Software version	CNR-IREA P-SBAS 28.1
Applied algorithm description	Parallel SBAS Interferometry Chain
Sensor	Sentinel 1 A
Date of measurement start	2020–01–11 T15:56:43
Date of measurement end	2024–09-22 T15:57:05
Number of dates	93
Used DEM	SRTM 1 arcsec
Mode	IW
Antenna side	Right
Relative orbit number	58
Orbit direction	ASCENDING
Number of looks azimuth	5
Number of looks range	20
Polarization	VV

a. AHP implementation.

The AHP was employed to develop a weighted evaluation system through the following steps:

1. Pairwise comparisons of criteria were conducted using Saaty's 1–9 scale (Singh et al., 2023) (Fig. 5).
2. Each criterion was standardized on a scale of 1–5 (Supp. Table 2).
3. The Consistency Ratio (CR) was computed to validate the pairwise comparison matrix using the formula: CR = CI/RI. Where CI is the Consistency Index and RI is the Random Index. Analysis proceeded only if CR < 0.10 (Sutadian et al., 2017).

b. Archaeological risk map generation.

The final risk score for each archaeological site was calculated in ArcGIS software using the formula:

a

	1	2	3	4	5
1	1.00	2.00	6.00	4.00
2	1.00	1	2.00	6.00	4.00
3	0.50	0.50	1	4.00	2.00
4	0.17	0.17	0.25	1	2.00
5	0.25	0.25	0.50	0.50	1

b

Cat		Priority	Rank	(+)	(-)
1	RSI	33.8%	1	5.1%	5.1%
2	LI	33.8%	1	5.1%	5.1%
3	DTWT(m)	18.3%	3	5.4%	5.4%
4	Soil Texture	7.1%	4	3.7%	3.7%
5	Subsidence	7.1%	5	2.1%	2.1%

Fig. 5. (a) Pairwise comparison matrix of criteria using Saaty's 1–9 scale and (b) the resulting weights for the criteria based on pairwise comparisons.

$$\text{Risk Score} = W_1(\text{RSI}) + W_1(\text{LI}) + W_2(\text{WTD}) + W_3(\text{ST}) + W_4(\text{LS})$$

Where W_1, W_2, W_3, and W_4 are the weights derived from the AHP analysis. Sites were classified into four risk categories based on the risk scores: Low risk, Moderate risk, High risk, and Severe risk.

3.6. Geostatistical analysis

Hydrochemical indices, P-SBAS displacement values, and risk scores were interpolated using the Kriging method in ArcGIS software version 10.7.1. This method is based on the spatial autocorrelation structure of the data, allowing for the prediction of values in areas where direct measurements are unavailable (Madani et al., 2022). Kriging preserves actual observed patterns, providing a comprehensive spatial representation of the study area (Orellana et al., 2023). This technique offers reliable predictions at unsampled locations, making it an effective tool for spatial analysis (Ikuemonisan et al., 2020).

4. Results and discussion

This section presents the analysis of saltwater intrusion and land subsidence affecting archaeological sites in the northeastern Nile Delta. We began by examining the hydrochemical processes and groundwater genesis. We then analyzed groundwater salinization and its corrosion potential. Next, we used SAR data to investigate land subsidence and its impact on site deterioration. Lastly, we employed multi-criteria analysis using the AHP method, based on corrosion indices, water table depth, soil texture, and subsidence, to create a risk degree map, identifying sites needing urgent mitigation strategies.

4.1. Hydrochemical processes and groundwater genesis

The Chadha diagram classified 80.7 % of the groundwater samples as seawater (Na—Cl type), indicating the dominant hydrogeochemical processes affecting groundwater chemistry (Supp. Table 3). The spatial distribution map of hydrochemical processes clearly illustrated the prevalence of seawater intrusion in the northern and central regions (Fig. 6a, b). These results provide compelling evidence that saltwater intrusion is the primary hydrochemical process influencing and altering groundwater chemistry (Ghosh and Jha, 2023; Perumal et al., 2024). This indicates that groundwater mineralization is predominantly attributed to the mixing of encroaching saline water from the sea, rather than natural rock weathering or other geological processes (Chaillou et al., 2018; Sidibe et al., 2019).

The Sulin diagram was used to classify groundwater genesis into four distinct types (Supp. Table 3): old marine water in the northern region,

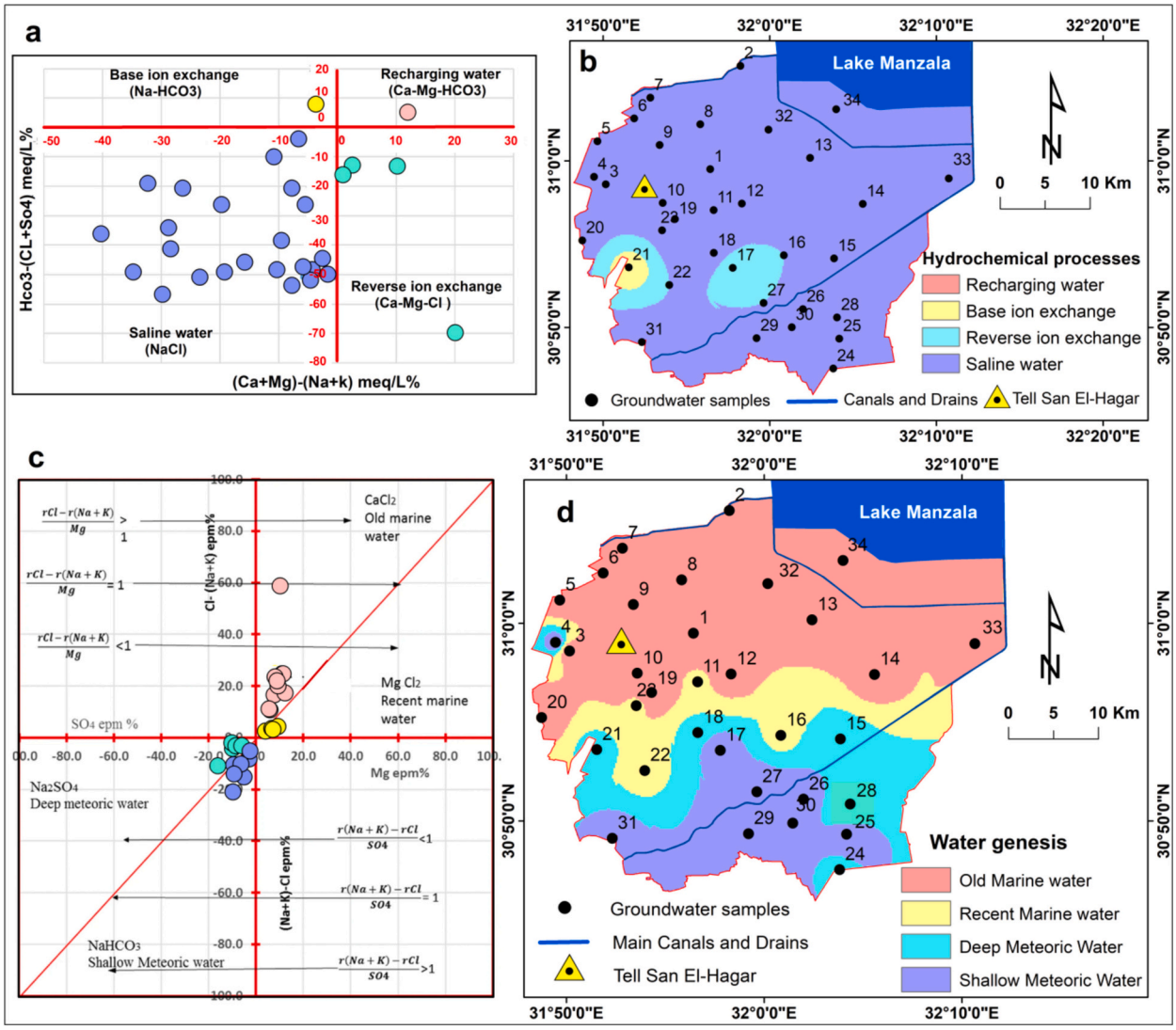

Fig. 6. Hydrochemical processes and water genesis in the shallow groundwater aquifer: (a) chadha diagram illustrating dominant hydrogeochemical processes; (b) spatial distribution map of dominant processes; (c) sulin diagram categorizing water genesis types; and (d) spatial distribution map of groundwater origin types.

recent marine water in the central region, and both shallow and deep meteoric water in the southern area (Fig. 6c, d).

The prevalence of "old marine water" in the northern region indicates a significant influence of paleo-marine water on the current groundwater composition, suggesting a long residence time within the aquifer. This aligns with the historical context provided by Hagage et al. (2023a), who reported that the northeastern Nile Delta was submerged under seawater between 7000 and 3000 BCE (Appendix A. Fig. 1a). Subsequently, between 500 and 1000 CE, the shoreline retreated, leading to the formation of Lake Manzala due to severe subsidence (Appendix A. Fig. 1b). The area remained submerged by Lake Manzala until the 1970s (Appendix A. Fig. 1c). In the 1980s, agricultural reclamation efforts intensified in the northeastern Nile Delta, especially after the construction of the El-Salam Canal. This canal served as a hydraulic barrier, diverting Lake Manzala's water from advancing southward, resulting in the lake's shrinkage and agricultural expansion south of the canal (Appendix A. Fig. 1d) (Hagage et al., 2023a). This historical submersion explains the presence of "old marine water" in the northern region, as the groundwater in this area has retained characteristics of ancient seawater that once covered the region.

The distribution of "recent marine water" in the central region indicates modern marine influences on groundwater, confirming ongoing seawater intrusion processes due to sea-level rise and groundwater overexploitation (Attwa et al., 2016; Abu Salem et al., 2022; Abdelfattah et al., 2023). Conversely, the presence of "shallow and deep meteoric water" in the southern area indicates recent recharge from surface drainage, canals, and irrigation return flows (El-Sayed et al., 2018; El-Aassar et al., 2023).

Previous studies of seawater intrusion in the eastern Nile Delta (e.g., Attwa et al., 2016; Abd-Elhamid, 2017; Mabrouk et al., 2018; Abu Salem et al., 2022; Taha et al., 2023; Abdelfattah et al., 2023) attributed saltwater intrusion primarily to contemporary factors such as rising sea levels and excessive groundwater extraction. In contrast, our findings offer valuable insights by distinguishing between historical and ongoing contemporary saltwater intrusion.

The results affirm that seawater intrusion is not a recent phenomenon in the eastern Nile Delta aquifer but has influenced groundwater chemistry since ancient times, with the historical seawater submersion and subsequent Lake Manzala formation in the north providing clear evidence of northern groundwater's ancient marine origin.

4.2. Groundwater salinization and corrosion potential

4.2.1. Assessment of groundwater salinization

To evaluate the degree of groundwater salinization at archaeological sites, we calculated three hydrochemical indices: seawater fraction (f_{sea}), Groundwater Quality Index for Seawater Intrusion (GQ_{ISWI}), and the Hydrochemical Facies Evolution Diagram (HFE-Diagram). These

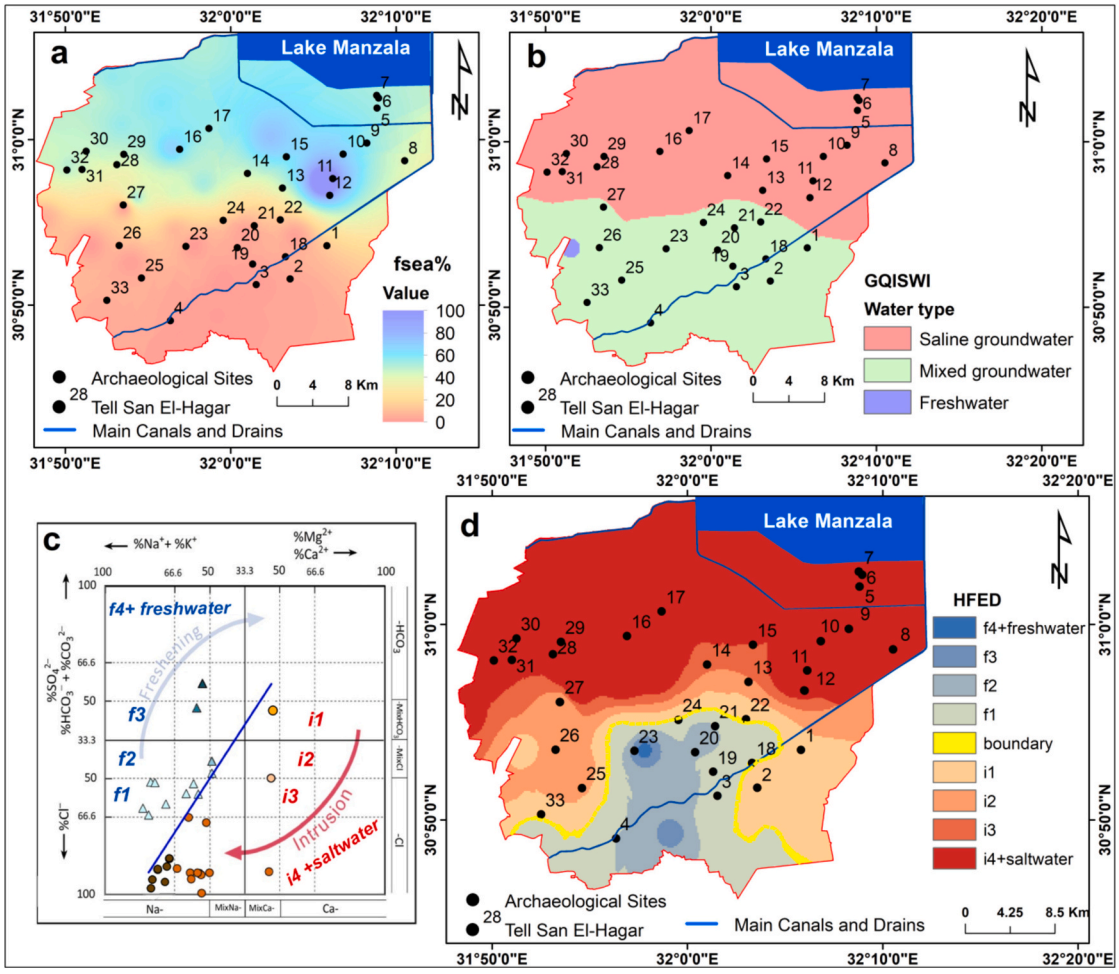

Fig. 7. Spatial distribution maps illustrating the degree of seawater intrusion in archaeological sites: (a) seawater fraction (f_{sea}) indicating the percentage contribution of seawater to groundwater, where higher values represent greater seawater influence; (b) Groundwater Quality Index for Seawater Intrusion (GQI_{SWI}), classifying groundwater quality from fresh to saline; (c) hydrochemical Facies Evolution (HFE) diagram showing the distribution of groundwater samples along the seawater intrusion and freshening phases; (d) spatial distribution of seawater intrusion dynamics derived from the HFE diagram, distinguishing between seawater intrusion and freshening phases.

indices were chosen for their ability to quantify the extent of seawater intrusion and classify groundwater types based on their chemical composition. Supp. Table 4 presents the calculated values of these indices.

The f_{sea} results revealed that the seawater contribution to groundwater ranged from 1 % to 82 %, with an average of 29 %. This contribution increased northward, indicating a gradient of seawater intrusion. The spatial distribution map for f_{sea} (Fig. 7a) shows that the seawater contribution to groundwater exceeded 50 % in all northern archaeological sites, highlighting the severity of the intrusion in these areas.

The GQI_{SWI} categorized the groundwater samples as 48.4 % saline water, 45.2 % mixed water, and 6.4 % freshwater. The spatial distribution map for GQISWI (Fig. 7b) indicates that 54.6 % of the archaeological sites had saline groundwater, and 45.4 % had mixed groundwater, underscoring the widespread impact of seawater intrusion on archaeological sites.

The HFE diagram, which tracks the progression of seawater intrusion through distinct chemical stages, offers a more nuanced view of the seawater intrusion process, dividing groundwater in archaeological sites into two main groups: those on the right side of the mixing line indicate the seawater intrusion phase, while those on the left side indicate the freshening phase (Fig. 7c). The diagram further subdivides these phases into stages, from f1 to f4 + FW for the freshening process and from i1 to i4 + SW for the intrusion process. The spatial distribution HFE map (Fig. 7d) reveals a northward intrusion pattern, with groundwater in the north reaching the i4 + SW sub-stage, indicating that the intrusion has progressed to its final phase in these areas. This diagram also shows that the current freshwater-seawater interface is located in the southernmost part of the study area, with 73 % of archaeological sites positioned north of this interface, resulting in highly saline groundwater conditions at the majority of study sites.

Collectively, the f_{sea}, GQI_{SWI}, and HFE-Diagram results indicated that archaeological sites in the northern and central regions of the study area contained highly saline groundwater, with salinity levels increasing towards the north. This situation is concerning given the shallow water table in these areas, which reached 0.6 m below the surface in the northeastern region (Fig. 2a). Such conditions facilitate direct interactions between archaeological sites and hypersaline groundwater.

4.2.2. Evaluation of scaling and corrosion potential

To determine the potential impacts of shallow saline groundwater on archaeological sites, the scaling and corrosion potential were evaluated using two indices: the Ryznar Stability Index (RSI) and the Larson-Skold Index (LI). These indices assess the groundwater's ability to dissolve or precipitate calcium carbonate ($CaCO_3$) and its corrosiveness relative to different surfaces. The computed values for these indices are presented in Supp. Table 5.

The RSI values ranged from 5.21 to 8.67, indicating diverse groundwater-archaeological site interactions. The RSI map (Fig. 8a) shows that 54.8 % of the samples have a light scaling tendency, 29 % exhibit little scaling/corrosion tendency, 6.6 % display significant corrosion tendency, and 9.6 % show heavy corrosion tendency. This variability suggests that archaeological sites are exposed to different forms of interaction with groundwater, from calcium carbonate accumulation on archaeological feature surfaces in the western region to severe corrosion of calcium carbonate-based features in the eastern area.

The accumulation of calcium carbonate coatings on archaeological features in the western region can cause irreversible physical and aesthetic damage, including changes in surface morphology, obscuring of inscriptions, and covering of decorative details over time (Hagage, 2021; Sáenz-Martínez et al., 2021; Vallet et al., 2022). On the other hand, corrosion tendencies in the eastern area pose a severe threat to calcium carbonate artifacts and structures, which is particularly concerning given that calcium carbonate is a primary component of many artifacts discovered in the study area (Abdulaziz, 2019; Gaber et al., 2021; El-Hassan and Abd El-Tawab, 2023).

Meanwhile, the LI values ranged from 947.6 to 0.83, with an average of 107. All samples, except for two, were classified as highly corrosive to different surfaces due to high concentrations of chloride and sulfate resulting from seawater intrusion. The LI spatial distribution map (Fig. 8b) demonstrates the highly aggressive nature of groundwater across all archaeological sites, suggesting a significant corrosive impact on archaeological building materials that could potentially lead to their complete deterioration over time. Corrosion can result in changes in

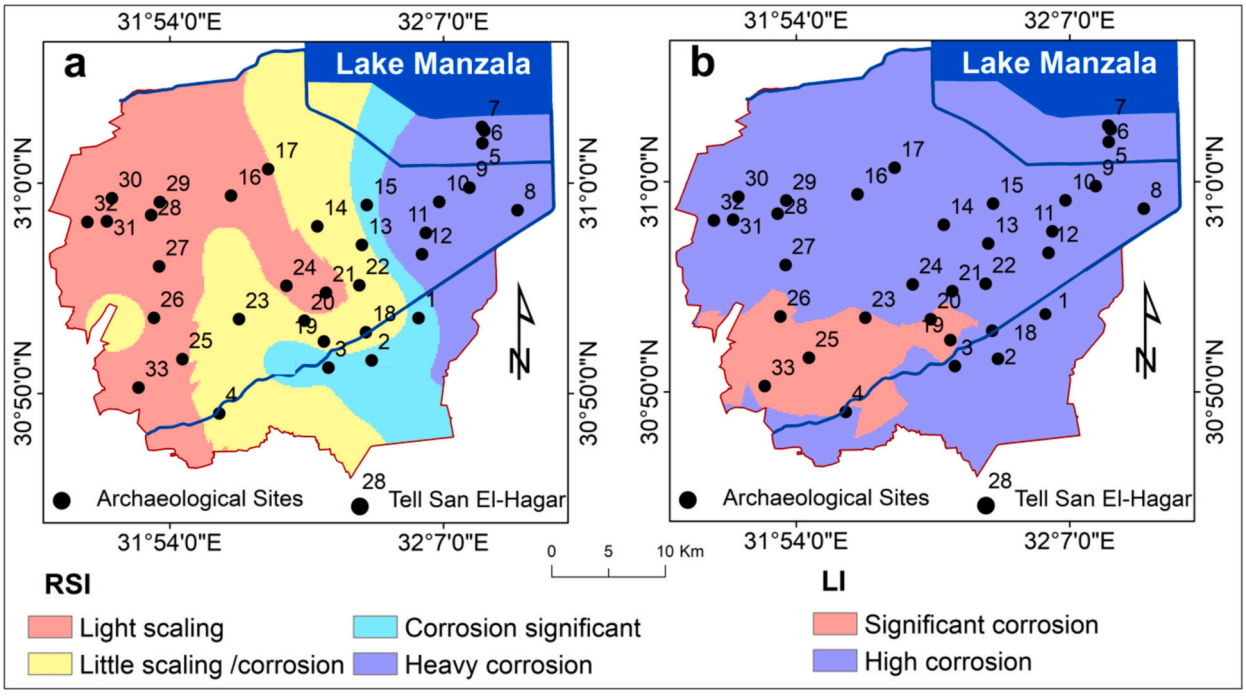

Fig. 8. Spatial distribution maps of groundwater corrosion and scaling indices at archaeological sites: (a) Ryznar Stability Index (RSI), indicating scaling and corrosion tendencies of calcium carbonate; and (b) Larson-Skold Index (LI), depicting corrosion aggressiveness relative to different surfaces.

appearance, structural damage, and ultimately, complete deterioration of artifacts (Smith et al., 2003; Hagage et al., 2023b; El-Gohary, 2023).

4.2.3. Factors contributing to archaeological site deterioration

There are two primary factors that contribute to the accelerated deterioration of archaeological sites due to shallow saline groundwater in the study area: soil texture and the continuous rise in the water table.

The rising water table, which increases at a rate of 3 to 8 cm per year in the eastern Nile Delta (Mansour, 2012; Arnous et al., 2015), exacerbates the situation. This rise is due to various factors, including increased recharge from excess irrigation water, seepage from canals and drainage systems, reduced groundwater discharge to Lake Manzala following the construction of the El-Salam Canal, and decreased groundwater abstraction due to very high salinity levels (Hagage et al., 2023a). As a result, saline groundwater increasingly infiltrates archaeological tells, mobilizing soluble salts that trigger various deterioration mechanisms (Fahmy et al., 2022; Alsubaie et al., 2024).

Another factor is soil texture. Soil sample analysis from the study area at a depth of one meter revealed that clay texture dominates most of the study area (Fig. 9a). This facilitates capillary transport of salts from shallow groundwater into archaeological layers (Ayers and Westcot, 1985). This process is particularly rapid in irrigated arid climates like the study area, where high evaporation rates lead to salt accumulation in the soil (Cui et al., 2019; Lian et al., 2022) (Fig. 9b). The rate of soil salt accumulation is influenced by various factors, including groundwater depth and salinity, soil texture, and climate. In the study area, which is characterized by clay-rich soils and shallow groundwater levels, capillary flow likely operates at its maximum potential. This capillary rise of saline groundwater promotes evaporation of solutions at layer surfaces, leading to salt concentration that can damage various archaeological materials, including limestone, mudbrick, and organic remains (El-Shishtawy et al., 2013; Ahmed and Fogg, 2014; Fahmy et al., 2022; Hagage et al., 2023b).

Although excavation work has only been conducted in the western area of Tell San El-Hager, studies conducted at the site confirm the severe deterioration processes indicated by our results. For example, investigations of granite obelisks revealed granular disintegration, scaling, cracking, and loss of hieroglyphs attributed to chemical weathering by

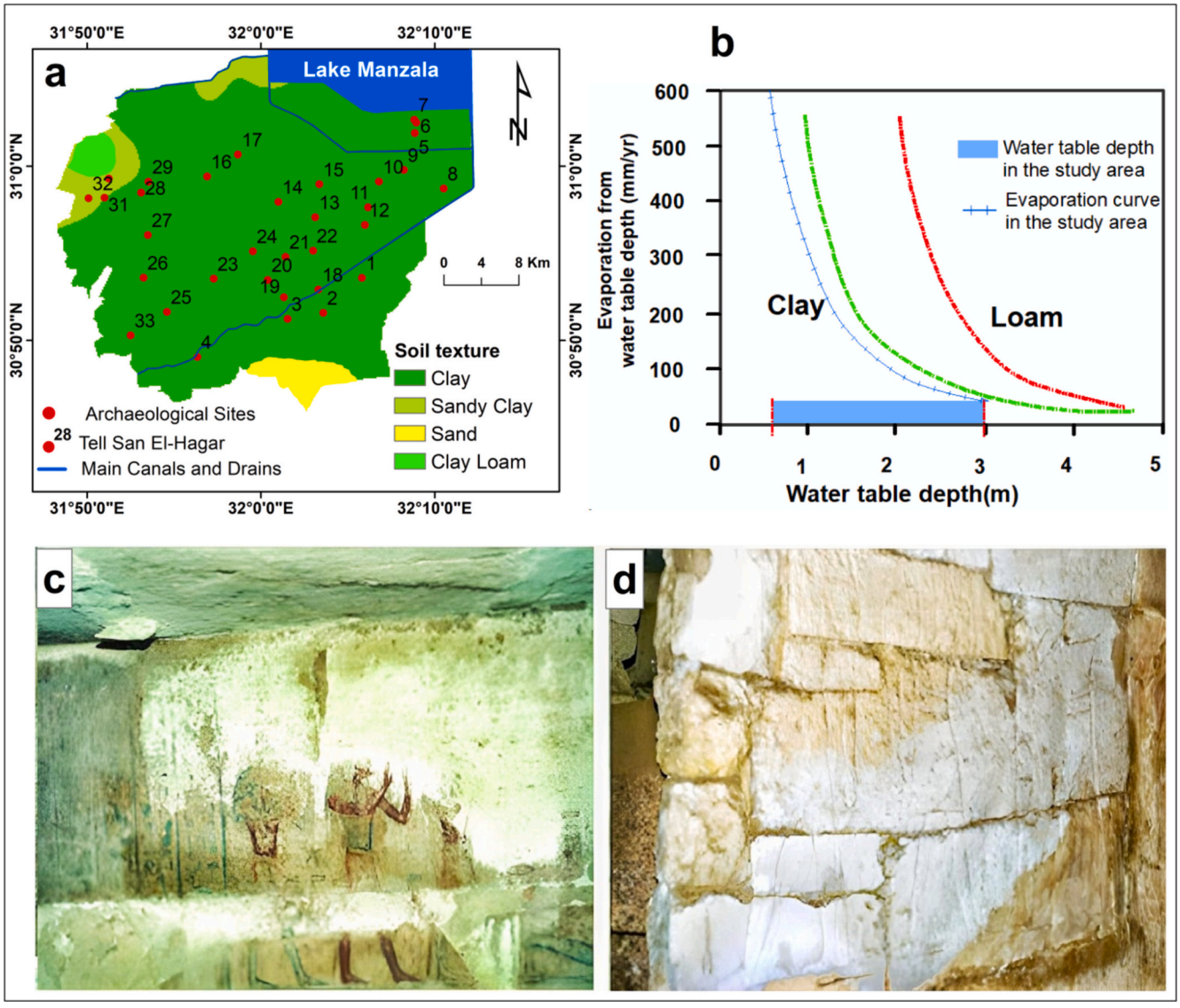

Fig. 9. (a) Soil texture map of the study area showing the distribution of different soil types and locations of archaeological sites, (b) relationship between water table depth and evaporation rate for different soil textures (Ram et al., 2008), illustrating the range of water table depths observed in the study area, (c) wall paintings in a royal tomb at Tell San El-Hagar showing discoloration and deterioration due to salt crystallization, and (d) Limestone wall in a royal tomb displaying severe cracking and surface degradation caused by salt-induced weathering (c and d adapted from El-Hassan and Abd El-Tawab, 2023).

saline groundwater (Helmi and Hefni, 2016). Vallet et al. (2022) identified chloride and sulfate salts as primary sources of deterioration at the same site, leading to issues such as gaps, chipping, cracks, and white calcium carbonate coatings on surfaces. Studies on the royal tombs (Fig. 9c, d) uncovered significant salt-induced damage, including loss of cohesion from salt crystallization, micro-cracks, and corrosion primarily by halite (NaCl) and gypsum ($CaSO_4 \bullet 2H_2O$) salts (El-Hassan and Abd El-Tawab, 2023).

4.3. Land subsidence and its implications

To investigate land subsidence, a dataset comprising 93 Sentinel-1 acquisitions from 2020 to 2024 was processed. This extensive dataset yielded a total of 20,999 measurement points, providing comprehensive coverage of the study area, with the exception of water bodies located in the northeast.

The results revealed Line-of-Sight (LOS) displacement velocities ranging from −16 mm/year to +5 mm/year (Fig. 10a). To address spatial data gaps, particularly over water bodies, Kriging interpolation was employed to predict displacement values for locations not identified by the SBAS-InSAR analysis (Fig. 10b). The resulting interpolation map demonstrated that maximum subsidence was concentrated in the northern region, where 8 archaeological sites are situated.

Land subsidence in the Nile Delta region results from a combination of natural phenomena and anthropogenic activities. Natural factors include the compaction of thick Holocene sediments and tectonic movements, while human-induced factors comprise groundwater overpumping, natural gas extraction, and urbanization (Gebremichael et al., 2018; Saleh and Becker, 2019; Rateb and Abotalib, 2020; Abd El-Hamid et al., 2023). Additionally, the construction of the Aswan High Dam has contributed to subsidence by reducing sediment supply to the Delta (Stanley and Clemente, 2017). In the study area, where extreme groundwater salinity severely constrains its use, subsidence is predominantly driven by natural factors rather than human activities.

Subsidence exacerbates archaeological degradation through two primary mechanisms: accelerating saltwater intrusion from the sea and Lake Manzala, and contributing to rising water table levels. While previous studies on saltwater intrusion in the Nile Delta have predominantly examined the impacts of sea level rise and excessive groundwater extraction (Abd-Elhamid, 2017; Mabrouk et al., 2018; Abd-Elaty et al., 2023; Abdelfattah et al., 2023; Taha et al., 2023), the role of land subsidence in exacerbating this issue has been largely overlooked. Subsidence compounds the effects of rising sea levels by diminishing land elevations, facilitating further incursion of seawater (Chala et al., 2022). Moreover, subsidence can disrupt hydraulic gradients and alter groundwater flow paths, potentially hastening the intrusion of saline water into freshwater aquifers (Acuña-Lara et al., 2020; Lu et al., 2022). It also intensifies the infiltration of saltwater into surface water bodies connected to aquifers (Cantelon et al., 2022). Furthermore, subsidence may lead to increased groundwater levels beneath the soil surface, particularly in regions where groundwater extraction is reduced and irrigation water recharge is heightened, as observed in the study area.

The risks stemming from saltwater intrusion and land subsidence in the Nile Delta are anticipated to escalate due to climate change and global sea level rise (Stanley and Clemente, 2017), leading to a depletion of usable freshwater resources and heightened risks of corrosion to archaeological heritage. Global sea level rise has undergone significant acceleration, increasing from 1.4 mm per year in the 20th century to over 3.6 mm per year since 2006. As of 2022, the global average sea level was recorded at 101.2 mm above the 1993 levels (Lindsey, 2021). Current projections suggest that by 2100, the average sea level could increase by 65 cm, primarily due to climate change (Gregory et al., 2019; Rezvi et al., 2023). This persistent upward trend is anticipated to continue for centuries owing to the continual warming of oceans and the

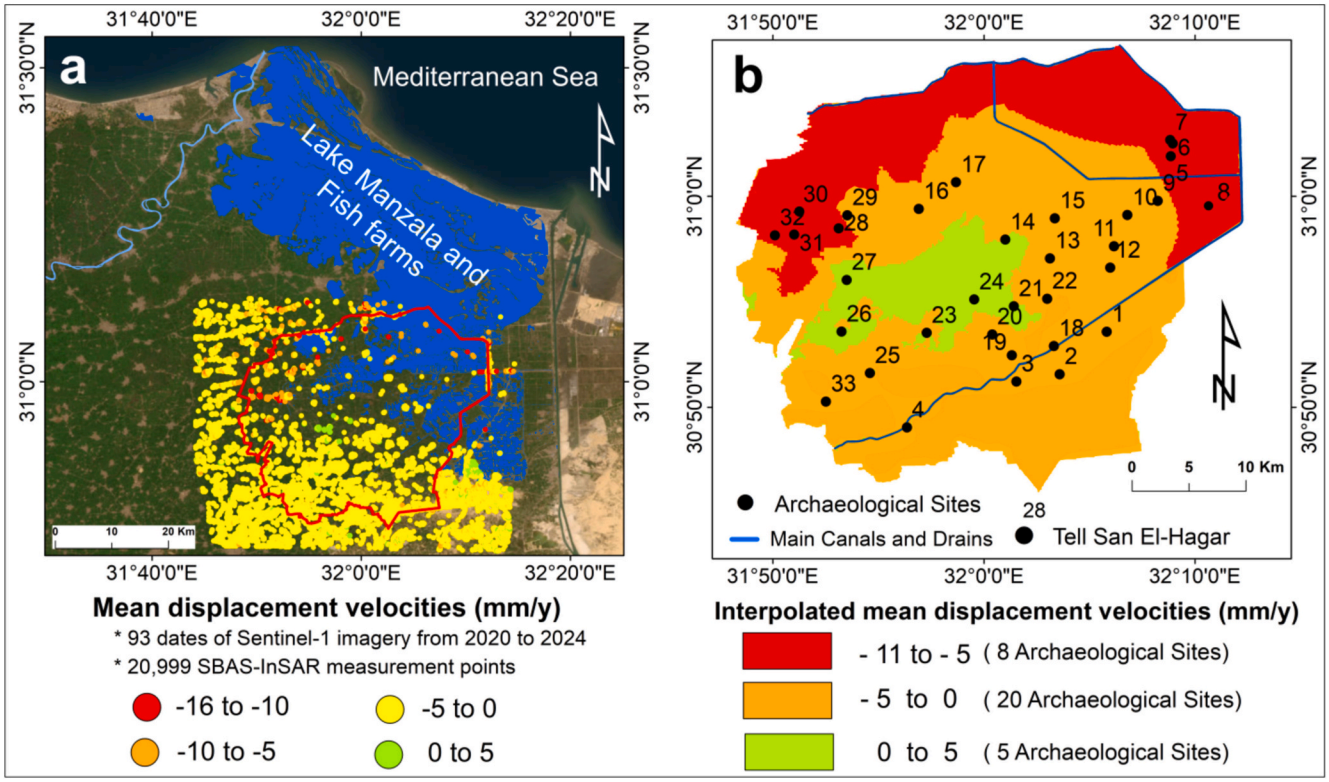

Fig. 10. Land subsidence analysis in the study area: (a) spatial distribution of mean Line-of-Sight (LOS) displacement velocities (mm/year) derived from SBAS-InSAR processing of Sentinel-1 data (2020–2024). Negative values indicate subsidence, while positive values represent uplift. (b) Interpolated map of mean LOS velocities generated through Kriging of SBAS-InSAR measurement points. This map provides continuous coverage of displacement rates across the study area, including regions where direct InSAR measurements were not available.

atmosphere, consequently heightening the risk of seawater intrusion (Tran et al., 2024).

Archaeological sites in the northern part of the study area, characterized by low-lying terrain and high subsidence rates, are particularly vulnerable to sea level rise risks. Rising sea levels will drive the freshwater-seawater interface inland, leading to the submergence of more archaeological tells in saline groundwater, waterlogging, and soil salinization caused by rising saline water tables (Vousdoukas et al., 2022; Abd El-Hamid et al., 2023; Lü et al., 2023). These changes may return the northeastern Nile Delta to an ancient inundated wetland environment, reminiscent of conditions 1500 years ago when subsidence gave rise to Lake Manzala and sabkha mudflats (Pennington et al., 2017; Hagage et al., 2023a) (Appendix A. Fig. 1). This transformation could render a significant portion of the presently inhabited and cultivated land in the north of the study area as unproductive marshland unsuitable for human habitation.

4.4. Archaeological risk map and mitigation strategies

4.4.1. Risk map development

To assess the vulnerability of archaeological sites to groundwater-induced deterioration, this study employed the Analytical Hierarchy Process (AHP) method, integrating four key factors: groundwater corrosion indices, water table depth, soil texture, and subsidence rates. The AHP analysis involved 33 archaeological sites across the study area. Each factor was weighted based on its relative importance in contributing to archaeological deterioration, as determined through pairwise comparison matrices verified by consistency ratio calculations. The weighting results indicated that corrosion indices carried the highest significance, followed by water table depth, soil texture, and subsidence rate. The consistency ratio was calculated as 0.042, well within the acceptable range of <0.1, confirming the reliability of the weightings (Singh et al., 2023).

Using these weighted criteria, a comprehensive risk map was generated through ArcGIS software version 10.7.1. The resulting map classified archaeological sites into four risk categories: low, moderate, high, and severe. Analysis revealed that 8 sites fall within the severe risk category, 12 sites in high risk, 11 sites in moderate risk, and only 2 sites in the low risk category (Fig. 11).

Spatially, the highest risk sites were predominantly concentrated in the north of the study region, where the combination of shallow water tables, high subsidence rates, and extreme corrosion potential created particularly hazardous conditions for archaeological preservation. The 8 sites in the northeast were identified as facing the most severe risks. The risk map shows that Tell San El-Hagar is located in a high-risk area, which is consistent with the documented deterioration at Tell San El-Hagar by El-Hassan and Abd El-Tawab (2023) and Vallet et al. (2022), supporting the reliability of our assessment methodology.

4.4.2. Suggested Mitigation strategies

Based on our risk assessment results, we propose a multi-approach mitigation strategy including expediting the discovery of archaeological sites in the severe risk category, lowering the water table to minimize contact between shallow saline groundwater and archaeological sites in high-risk areas, and developing regular monitoring programs for moderate and low-risk sites.

A. Severe risk areas (Urgent excavation sites).

Areas exposed to severe degradation are concentrated in the northeast of the study area and include eight archaeological sites. The proposed mitigation strategy will be implemented in two stages:

1. Implementation of local dewatering systems: This includes lowering the water table by constructing pumping wells around the archaeological sites. Carefully managed pumping has been shown to be effective in lowering local groundwater levels at archaeological sites (Campos, 2009; Hassan et al., 2012).
2. Urgent archaeological surveys: These will use geophysical techniques such as ground-penetrating radar (GPR) and electrical resistivity tomography (ERT) to identify and extract subsurface archaeological features (e.g., Ghazala et al., 2003; El-Kenawy et al., 2013; Gaber et al., 2021).

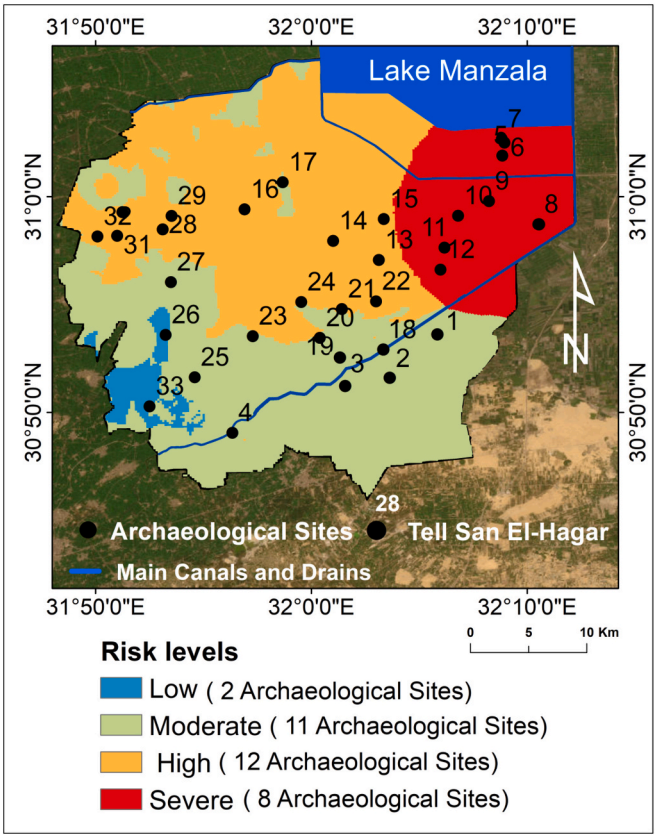

Fig. 11. Archaeological risk map: Distribution of groundwater-induced deterioration risk levels. The risk categories represent potential groundwater-related damage to archaeological sites, assessed using the Analytical Hierarchy Process (AHP) method by integrating groundwater corrosion indices, water table depth, soil texture, and subsidence rates.

B. High-Risk sites.

Areas exposed to high degradation are concentrated in the northwest of the study area and include twelve archaeological sites. The proposed strategy to mitigate degradation includes lowering shallow saline water tables to depths exceeding three meters, which is crucial for effectively reducing the capillary rise of salts (Ram et al., 2008). This can be achieved through the following strategies:

- Groundwater pumping (well pumping) for various uses: The advantages of this technique include providing direct and immediate control over groundwater levels (El-Fakharany and Fekry, 2014; Hagage et al., 2025). This technique has been successfully employed in various parts of the world to mitigate waterlogging and its associated problems (Deng and Bailey, 2020; Singh, 2024).
- Implementation of subsurface drainage systems: Particularly in areas where water tables are less than one meter below the surface (Kaiser et al., 2013; Sojka et al., 2019; Hammam and Mohamed, 2020).
- Using efficient irrigation techniques: In agricultural areas surrounding archaeological sites, this can help reduce excess recharge from irrigation water to groundwater (Ahmed and Fogg, 2014).

Using drip irrigation or precision sprinkler systems could significantly decrease water input while maintaining crop yields (Kaur et al., 2020).

- Lining canals with impermeable materials: Especially near the El-Salam Canal, this will help reduce water seepage into the groundwater and minimize local rises in the water table (Elkamhawy et al., 2021; Abd-Elziz et al., 2022).
- Bio-pumping (also known as bio-drainage): It is an innovative strategy that employs deep-rooted vegetation to lower groundwater levels and manage waterlogging (Singh and Lal, 2018). This eco-friendly approach involves planting fast-growing tree species that absorb excess soil water through their roots and transpire it into the atmosphere, effectively reducing the water table (Ram et al., 2008).

By implementing these strategies, we can effectively manage groundwater salinization and protect archaeological sites from degradation.

5. Conclusion and recommended additional studies

This study presents the first assessment of groundwater salinization and land subsidence impacts on archaeological sites in the northern Nile Delta, addressing a critical gap in previous research. Our multi-methodological approach, combining hydrochemical investigations, InSAR techniques, and multi-criteria decision analysis, has yielded significant insights into the threats facing this invaluable cultural heritage.

Key findings reveal that 80.7 % of groundwater samples are classified as seawater (Na—Cl type), with saltwater intrusion being the primary influence on groundwater chemistry. The study identified four distinct water types, with old marine water predominating in the northern region. This demonstrates that seawater intrusion in the eastern Nile Delta aquifer is a long-standing phenomenon rather than a recent development, evidenced by paleo-marine influences in the northern region and modern marine influences in the central region.

Groundwater quality assessments indicated that 54.6 % of archaeological sites have saline groundwater, while 45.4 % have mixed groundwater. The current freshwater-seawater interface is located in the southernmost part of the study area, placing the majority of archaeological sites in highly saline groundwater zones with shallow water tables. This positioning exposes artifacts to direct contact with groundwater and capillary rise effects.

Groundwater corrosion and scaling indices revealed a high risk of limescale accumulation and corrosive conditions at all archaeological sites, primarily due to elevated chloride and sulfate concentrations from seawater intrusion. SBAS-InSAR analysis detected displacement velocities ranging from −16 mm/year to 5 mm/year, with maximum subsidence concentrated in the northern region, exacerbating saltwater intrusion and water table rise.

The archaeological risk map, developed using the Analytic Hierarchy Process, classified 8 sites as severe risk, 12 as high risk, 11 as moderate risk, and only 2 as low risk. The highest risk sites are predominantly in the north, where multiple adverse factors converge.

These findings underscore the urgent need for targeted conservation efforts and mitigation strategies. Proposed interventions include local dewatering systems, immediate archaeological surveys using geophysical techniques, lowering of shallow saline water tables, implementation of efficient irrigation techniques, and lining of canals with impermeable materials.

This study contributes significantly to the field by quantifying the combined threats to archaeological sites in the Nile Delta and providing a risk map to prioritize conservation efforts. However, further research is necessary to build upon these findings:

1- Assess the effectiveness of the proposed interventions through pilot studies and long-term observations.
2- Conduct economic evaluations of various preservation techniques to identify the most cost-effective and scalable solutions for different risk categories.
3- Investigate the potential effects of future climate scenarios on groundwater dynamics and land subsidence in the region.
4- Employ cutting-edge geophysical techniques to provide high-resolution subsurface imaging of archaeological sites, aiding in preservation planning.
5- Develop detailed numerical models to simulate future groundwater and land subsidence scenarios under various management strategies.

By addressing these research areas, future studies can build upon the foundation laid by this work, leading to more effective and sustainable preservation of the Nile Delta's rich archaeological heritage.

CRediT authorship contribution statement

Mohammed Hagage: Writing – original draft, Software, Methodology, Investigation, Data curation, Conceptualization. **Abdel Galil A. Hewaidy:** Writing – review & editing, Validation, Supervision, Methodology. **Abdulaziz M. Abdulaziz:** Writing – review & editing, Visualization, Conceptualization.

Consent to participate

All authors consent to participate.

Ethical approval

Not applicable.

Consent for publication

All authors consented to publish.

Funding

This research was conducted under project ID 3b11cK, supported by the ESA Network of Resources Initiative.

Declaration of competing interest

The authors declare that they have no known competing financial interests or personal relationships that could have appeared to influence the work reported in this paper.

Acknowledgements

This paper is part of the first author's PhD thesis. The authors gratefully acknowledge the support of the European Space Agency (ESA), as this research was conducted under project ID 3b11cK, supported by the ESA Network of Resources Initiative. We extend special thanks to Dr. Hervé Caumont for his exceptional technical support throughout our work on the Geohazards Thematic Exploitation Platform (Geohazards TEP).

Appendix A

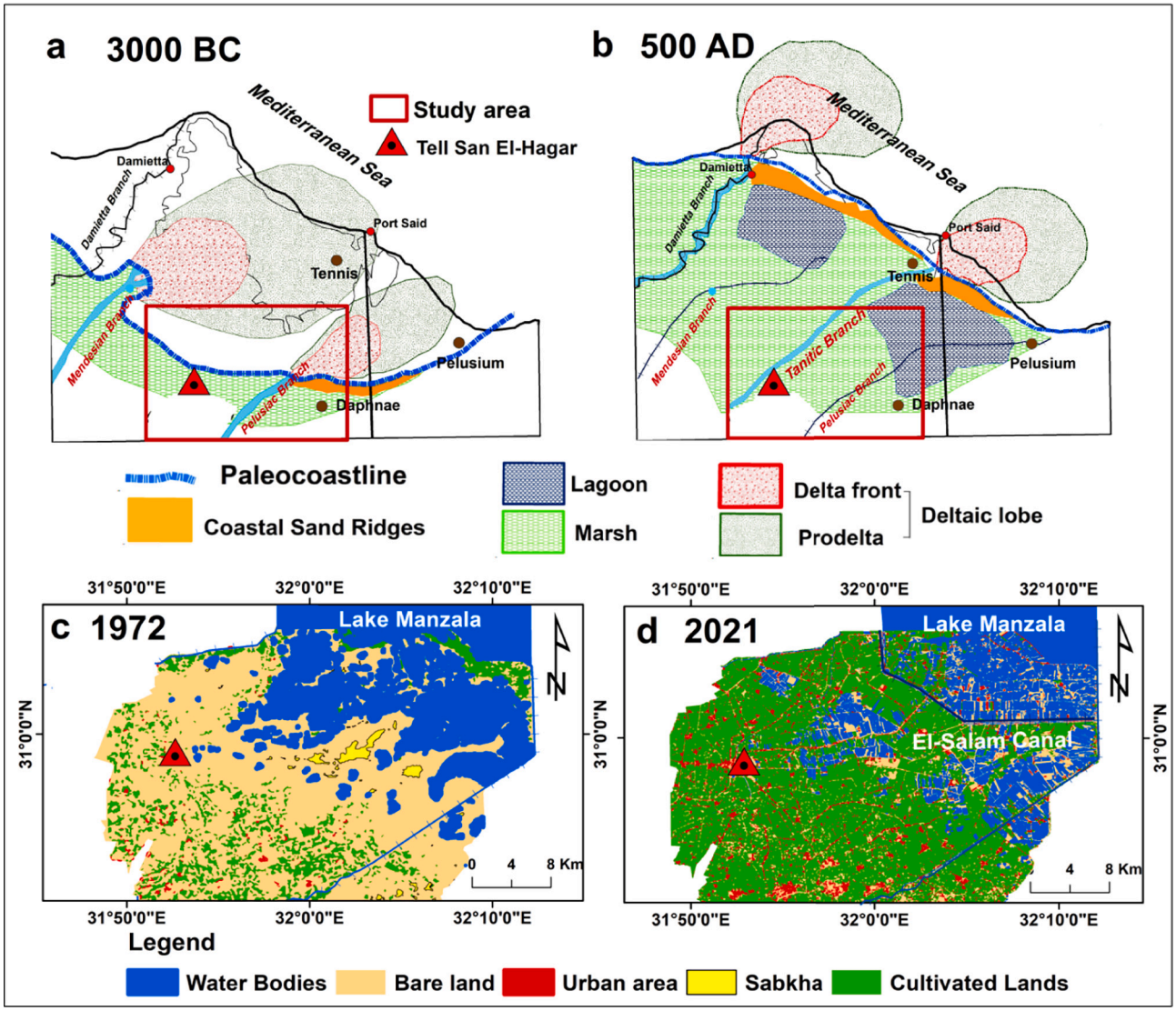

Appendix A. Fig. 1. Landscape evolution in the northeastern Nile Delta: (a) Historical map showing the area submerged under seawater (3000 BC); (b) formation of Lake Manzala (500 AD); (c) land cover in 1971 showing the extent of Lake Manzala; and (d) land cover in 2021 illustrating agricultural expansion and lake shrinkage following the construction of El-Salam Canal (adapted from Hagage et al., 2023a and Coutellier and Stanley, 1987)

Appendix B. Supplementary data

Supplementary data to this article can be found online at https://doi.org/10.1016/j.marpolbul.2024.117460.

Data availability

Data will be made available on request.

References

Abd El-Hamid, H.T., Alshehri, F., El-Zeiny, A.M., Nour-Eldin, H., 2023. Remote sensing and statistical analyses for exploration and prediction of soil salinity in a vulnerable area to seawater intrusion. Mar. Pollut. Bull. 187, 114555.

Abd-Elaty, I., Straface, S., Kuriqi, A., 2021. Sustainable saltwater intrusion management in coastal aquifers under climatic changes for humid and hyper-arid regions. Ecol. Eng. 171, 106382.

Abd-Elaty, I., Abdoulhalik, A., Ahmed, A., 2023. The impact of future hydrology stresses and climate change on submarine groundwater discharge in arid regions: A case study of the Nile Delta aquifer, Egypt. J. Hydrol. Region. Stud. 47, 101395.

Abdelfattah, M., Abdel-Aziz Abu-Bakr, H., Aretouyap, Z., Sheta, M.H., Hassan, T.M., Geriesh, M.H., Shaheen, S., Alogayell, H., EL-Bana, E., Gaber, A., 2023. Mapping the impacts of the anthropogenic activities and seawater intrusion on the shallow coastal aquifer of Port Said, Egypt. Front. Earth Sci. 11, 1204742.

Abdel-Fattah, M.K., 2019. Linear regression models to estimate exchangeable sodium percentage and bulk density of salt affected soils in Sahl El-Hossinia, El-Sharkia governorate, Egypt. Commun. Soil Sci. Plant Anal. 50 (16), 2074–2087.

Abd-Elhamid, H.F., 2017. Investigation and control of seawater intrusion in the eastern Nile Delta aquifer considering climate change. Water Sci. Technol. Water Supply 17 (2), 311–323.

Abd-Elziz, S., Zeleňáková, M., Kršák, B., Abd-Elhamid, H.F., 2022. Spatial and temporal effects of irrigation canals rehabilitation on the land and crop yields, a case study: the Nile Delta, Egypt. Water 14 (5), 808.

Abdulaziz, A.M., 2019. Subsurface characterization for groundwater management nearby the unfinished obelisk archeological site, Aswan governorate, Egypt. Open J. Geol. 9 (11), 839–860.

Abo-El-Fadl, M.M., 2013. Possibilities of groundwater pollution in some areas, east of Nile Delta, Egypt. Int. J. Environ. 1 (1), 1–21.

Abou El-Magd, I., Zakzouk, M., Ali, E.M., Foumelis, M., Blasco, J.M.D., 2024. Exploring the potentiality of InSAR data to estimate land subsidence of the Nile Delta. Egypt. J. Remote Sensing Space Sci. 27 (2), 342–355.
Abu Salem, H.S., Gemail, K.S., Junakova, N., Ibrahim, A., Nosair, A.M., 2022. An integrated approach for deciphering hydrogeochemical processes during seawater intrusion in coastal aquifers. Water 14 (7), 1165.
Acuña-Lara, F., Pacheco-Martinez, J., Luna-Villavicencio, H., Hernández-Marín, M., González-Cervantes, N., 2020. Infiltration of surface water through subsidence failure assessment applying electric prospecting, case Aguascalientes Valley, Mexico. Proc. Int. Assoc. Hydrol. Sci. 382, 5–9.
Ahmed, A.A., Fogg, G.E., 2014. The impact of groundwater and agricultural expansion on the archaeological sites at Luxor, Egypt. J. Afr. Earth Sci. 95, 93–104.
Ahmed, S., Sultan, M.W., Alam, M., Hussain, A., Qureshi, F., Khurshid, S., 2021. Evaluation of corrosive behaviour and scaling potential of shallow water aquifer using corrosion indices and geospatial approaches in regions of the Yamuna river basin. J. King Saud Univ. Sci. 33 (1), 101237.
Alsubaie, M.S., Almutery, S.B., Almoufleh, A.A., Khalil, M.M., Sallam, A., 2024. Architectural heritage conservation in the City of Qurh: assessing and stabilizing Islamic era mud brick structures. Mediter. Archaeol. Archaeom. 24 (1), 50–73.
Aly, M.H., Klein, A.G., Zebker, H.A., Giardino, J.R., 2012. Land subsidence in the Nile Delta of Egypt observed by persistent scatterer interferometry. Remote Sens. Lett. 3 (7), 621–630.
APHA, 2012. Standard methods for the examination of water and wastewater, 22nd edition edited by E. W. Rice, R. B. Baird, A. D. Eaton and L. S. Clesceri. American public health association (APHA), American Water Works Association (AWWA) and water environment federation (WEF), Washington, D.C., USA.
Arnous, M.O., El-Rayes, A.E., Green, D.R., 2015. Hydrosalinity and environmental land degradation assessment of the East Nile Delta region, Egypt. J. Coast. Conserv. 19, 491–513.
Attwa, M., Gemail, K., Eleraki, M., 2016. Use of Salinity and Resistivity Measurements to Study the Coastal Aquifer Salinization in a Semi-Arid Region: A Case Study in Northeast Nile Delta, Egypt. Environ. Earth Sci. 784.
Ayers, R.S., Westcot, D.W., 1985. Water Quality for Agriculture. Food and Agriculture Organization of the United Nations, Rome.
Azari, T., Tabari, M.M.R., 2024. An integrated approach based on HFE-D, GIS techniques, GQI SWI, and statistical analysis for the assessment of potential seawater intrusion: coastal multilayered aquifer of Ghaemshahr-Juybar (Mazandaran, Iran). Environ. Sci. Pollut. Res. 1–37.
Bai, Z., Wang, Y., Li, M., Sun, Y., Zhang, X., Wu, Y., et al., 2023. Land subsidence in the Singapore coastal area with long time series of TerraSAR-X SAR data. Remote Sens. 15 (9), 2415.
Baskaran, V., Sridharan, M., Saravanane, R., Mohan, S., 2022. Cognizance about sea water intrusion by chemical analysis in coastal aquifer of southeast coast of India. Int. J. Energy Water Resour. 1–12.
Becker, R.H., Sultan, M., 2009. Land subsidence in the Nile Delta: inferences from radar interferometry. The Holocene 19 (6), 949–954.
Bokhari, R., Shu, H., Tariq, A., Al-Ansari, N., Guluzade, R., Chen, T., et al., 2023. Land subsidence analysis using synthetic aperture radar data. Heliyon 9, e14690.
Campos, E., 2009. A groundwater flow model for water related damages on historic monuments—case study West Luxor Egypt. Vatten 65, 247–254.
Cantelon, J.A., Guimond, J.A., Robinson, C.E., Michael, H.A., Kurylyk, B.L., 2022. Vertical saltwater intrusion in coastal aquifers driven by episodic flooding: A review. Water Resour. Res. 58 (11), e2022WR032614.
Chaillou, G., Touchette, M., Buffin-Bélanger, T., Cloutier, C.A., Hétu, B., Roy, M.A., 2018. Hydrogeochemical evolution and groundwater mineralization of shallow aquifers in the bas-Saint-Laurent region, Québec, Canada. Can. Water Res. J. Revue Can. Des Ress. Hydriques 43 (2), 136–151.
Chala, D.C., Quinones-Bolanos, E., Mehrvar, M., 2022. An integrated framework to model salinity intrusion in coastal unconfined aquifers considering intrinsic vulnerability factors, driving forces, and land subsidence. J. Environ. Chem. Eng. 10 (1), 106873.
Costall, A.R., Harris, B.D., Teo, B., Schaa, R., Wagner, F.M., Pigois, J.P., J. P., 2020. Groundwater throughflow and seawater intrusion in high quality coastal aquifers. Sci. Rep. 1, 1–33.
Coutellier, V., Stanley, D., 1987. Late quaternary stratigraphy and paleogeography of the eastern Nile Delta, Egypt. Mar. Geol. 77, 257–275.
Cui, G., Lu, Y., Zheng, C., Liu, Z., Sai, J., 2019. Relationship between soil salinization and groundwater hydration in Yaoba oasis, Northwest China. Water 11 (1), 175.
Daito, K., Galloway, D.L., 2015. Preface: prevention and mitigation of natural and anthoropogenic hazards due to land subsidence. Proc. Int. Assoc. Hydrol. Sci. 372 (372), 555–557.
Dammag, B., Jian, D., Dammag, A.Q., 2024. Cultural heritage sites risk assessment and management using a hybridized technique based on GIS and SWOT-AHP in the Ancient City of Ibb, Yemen. International Journal of Architectural Heritage 1–36.
De Luca, C., Cuccu, R., Elefante, S., Zinno, I., Manunta, M., Casola, V., et al., 2015. An on-demand web tool for the unsupervised retrieval of Earth's surface Deformation from SAR data: the P-SBAS service within the ESA G-POD environment. Remote Sens. 7, 15630–15650.
De Luca, C., Bonano, M., Casu, F., Manunta, M., Manzo, M., Onorato, G., et al., 2018. The parallel SBAS-DInSAR processing chain for the generation of national scale sentinel-1 deformation time-series. Proc. Comp. Sci. 138, 326–331.
Deng, C., Bailey, R.T., 2020. Assessing causes and identifying solutions for high groundwater levels in a highly managed irrigated region. Agric. Water Manag. 240, 106329.
Deng, S., Yang, H., Chen, X., Wei, X., 2022. Probabilistic analysis of land subsidence due to pumping by biot poroelasticity and random field theory. J. Eng. Appl. Sci. 69 (1), 18.
Dieu, L.P., Cong-Thi, D., Segers, T., Hieu Ho, H., Nguyen, F., Hermans, T., 2022. Groundwater salinization and freshening processes in the Luy River coastal aquifer, Vietnam. Water 14, 2358.
Echogdali, F.Z., Boutaleb, S., Bendarma, A., Saidi, M.E., Aadraoui, M., Abioui, M., Sajinkumar, K.S., 2022. Application of analytical hierarchy process and geophysical method for groundwater potential mapping in the Tata basin, Morocco. Water 14 (15), 2393.
El-Aassar, A.H., Hagagg, K., Hussien, R., Oterkus, S., Oterkus, E., 2023. Integration of groundwater vulnerability with contaminants transport modeling in unsaturated zone, case study El-Sharqia, Egypt. Environ. Monit. Assess. 195 (6), 1–13.
Elbeih, S.F., Madani, A.A., Hagage, M., 2021. Groundwater deterioration in Akhmim District, upper Egypt: a remote sensing and GIS investigation approach. Egypt. J. Remote Sens. Space Sci. 24 (3), 919–932.
Elbeih, S.F., Hagage, M., Attia, W., Abd el-sadek, E., 2023. Using treated wastewater in groundwater recharge at Wadi El Farigh area, Egypt: GIS and remote sensing applications. In: Gad, A.A., Elfiky, D., Negm, A., Elbeih, S. (Eds.), Applications of Remote Sensing and GIS Based on an Innovative Vision . ICRSSSA 2022, Springer Proceedings in Earth and Environmental Sciences. Springer, Cham. https://doi.org/10.1007/978-3-031-40447-4_8.
El-Fakharany, Z., Fekry, A., 2014. Assessment of new Esna barrage impacts on groundwater and proposed measures. Water Sci. 28 (1), 65–73.
El-Gohary, M.A., 2023. The environmental factors affecting the archaeological buildings in Egypt,"IV deterioration by synergistic marine effects". Herit. Sci. 11 (1), 1–14.
El-Hassan, R.A., Abd El-Tawab, N.A., 2023. A multi-analytical study of building materials and deterioration products of the royal tombs to TANIS (san el-HAGAR). Int. J. Conserv. Sci. 14 (4), 1351–1366.
Elkamhawy, E., Zelenakova, M., Abd-Elaty, I., 2021. Numerical canal seepage loss evaluation for different lining and crack techniques in arid and semi-arid regions: A case study of the river Nile, Egypt. Water 13 (21), 3135.
El-Kenawy, A., Metwaly, M., Gemail, K., El-Raouf, A.A., 2013. Contribution of geoelectrical resistivity sounding for paleoenvironment assessment at Saft El-henna and tell El-Dab'a archaeological sites, eastern Nile Delta, Egypt. Explor. Geophys. 44 (4), 282–288.
El-Sayed, S.A., Morsy, S.M., Zakaria, K.M., 2018. Recharge sources and geochemical evolution of groundwater in the quaternary aquifer at Atfih area, the northeastern Nile Valley, Egypt. J. Afr. Earth Sci. 142, 82–92.
El-Shishtawy, A.M., Atwia, M.G., El-Gohary, A., Parizek, R.R., 2013. Impact of soil and groundwater corrosion on the Hierakonpolis Temple town archaeological site, Wadi Abu Sufian, Idfu, Egypt. Environ. Monit. Assess. 185, 4491–4511.
ESA. (2023). Interferometric Wide Swath. Retrieved from sentinels.copernicus.eu: https://sentinels.copernicus.eu/web/sentinel/user-guides/sentinel-1-sar/acquisition-modes/interferometric-wide-swath.
Ezzeldin, H.A., 2022. Delineation of salinization and recharge sources affecting groundwater quality using chemical and isotopic indices in the northwest coast, Egypt. Sustainability 14 (24), 16923.
Fahmy, A., Molina-Piernas, E., Martínez-López, J., Domínguez-Bella, S., 2022. Salt weathering impact on Nero/Ramses II Temple at El-Ashmonein archaeological site (Hermopolis magna), Egypt. Herit. Sci. 10 (1), 125.
Foumelis, M., Delgado Blasco, J., Brito, F., Pacini, F., Papageorgiou, E., Pishehvar, P., et al., 2022. SNAPPING services on the Geohazards exploitation platform for Copernicus Sentinel-1 surface motion mapping. Remote Sens. 14 (23), 6075.
Gaber, A., Gemail, K.S., Kamel, A., Atia, H.M., Ibrahim, A., 2021. Integration of 2D/3D ground penetrating radar and electrical resistivity tomography surveys as enhanced imaging of archaeological ruins: A case study in San El-Hager (Tanis) site, northeastern Nile Delta, Egypt. Archaeol. Prospect. 28 (2), 251–267.
Gambolati, G., Teatini, P., 2015. Geomechanics of subsurface water withdrawal and injection. Water Resour. Res. 51 (6), 3922–3955.
Gebremichael, E., Sultan, M., Becker, R., El Bastawesy, M., Cherif, O., Emil, M., 2018. Assessing land deformation and sea encroachment in the Nile Delta: A radar interferometric and inundation modeling approach. J. Geophys. Res. Solid Earth 123 (4), 3208–3224.
Ghazala, H., El-Mahmoudi, A.S., Abdallatif, T.F., 2003. Archaeogeophysical study on the site of tell Toukh El-Qaramous, Sharkia governorate, East Nile Delta, Egypt. Archaeol. Prospect. 10 (1), 43–55.
Ghosh, S., Jha, M.K., 2023. Hydrogeochemical Characterization of Groundwater and Critical Assessment of its Quality in a Coastal Basin. Environ. Dev. Sustain. 1–66.
Gimenez-Forcada, E., 2019. Use of the Hydrochemical facies diagram (HFE-D) for the evaluation of salinization by seawater intrusion in the coastal Oropesa plain: comparative analysis with the coastal Vinaroz plain, Spain. HydroResearch 48 (2), 76–84.
Giménez-Forcada, E., Vega-Alegre, M., Timón-Sánchez, S., 2017. Characterization of regional cold-hydrothermal inflows enriched in arsenic and associated trace-elements in the southern part of the Duero Basin (Spain), by multivariate statistical analysis. Sci.Total Environ. 211–226.
Gregory, J.M., Griffies, S.M., Hughes, C.W., et al., 2019. Concepts and terminology for sea level: mean, variability and change, both local and global. Surv. Geophys. 40, 1251–1289.
Hagage, M. (2021). Impacts of Anthropogenic Activities on the Deterioration of Groundwater and Archaeological Sites in Akhmim Area, Sohag Governorate, Egypt: Remote Sensing and GIS Applications. M.Sc. Cairo University Egypt, Cairo.
Hagage, M., Madani, A.A., Elbeih, S.F., 2022. Quaternary groundwater aquifer suitability for drinking in Akhmim, upper Egypt: an assessment using water quality index and GIS techniques. Arab. J. Geosci. 15 (2), 196.

Hagage, M., Abdulaziz, A., Hewaidy, A., Shetaia, S., 2023a. Unveiling the past: utilizing satellite imagery archives to study archaeological landscapes in the northeastern Nile Delta, Egypt. Anthropocene 44, 100409.
Hagage, M., Hewaidy, A.G.A., Abdulaziz, A.M., 2025. Groundwater quality assessment for drinking, irrigation, aquaculture, and industrial uses in the waterlogged northeastern Nile Delta, Egypt: a multivariate statistical approach and water quality indices. Model Earth Syst. Environ. 11 (1), 1–15.
Hagage, M., Madani, A.A., Aboelyamin, A., Elbeih, S.F., 2023b. Urban sprawl analysis of Akhmim city (Egypt) and its risk to buried heritage sites: insights from geochemistry and geospatial analysis. Herit. Sci. 11 (1), 174.
Hagage, M., Abdulaziz, A.M., Elbeih, S.F., Hewaidy, A.G.A., 2024. Monitoring soil salinization and waterlogging in the northeastern Nile Delta linked to shallow saline groundwater and irrigation water quality. Sci. Rep. 14 (1), 27838.
Hajji, S., Allouche, N., Bouri, S., Aljuaid, A., Hachicha, W., 2022. Assessment of seawater intrusion in coastal aquifers using multivariate statistical analyses and hydrochemical facies evolution-based model. Int. J. Environ. Res. Public Health 19 (1), 155.
Hakim, W., Achmad, A., Eom, J., Lee, W., 2020. Land subsidence measurement of Jakarta coastal area using time series interferometry with Sentinel-1 SAR data. J. Coast. Res. 102, 75–81.
Hammam, A.A., Mohamed, E.S., 2020. Mapping soil salinity in the East Nile Delta using several methodological approaches of salinity assessment. Egypt. J. Remote Sens. Space Sci. 23 (2), 125–131.
Hasan, S.S., Salem, Z.E., Sefelnasr, A., 2023. Assessment of Hydrogeochemical characteristics and seawater intrusion in coastal aquifers by integrating statistical and graphical techniques: quaternary aquifer, West Nile Delta, Egypt. Water 15 (10), 1803.
Hassan, N.A., Kotb, A., Hassan, A.A., Hagras, M.A., 2012. Dewatering using groundwater modelling in Al-Fustat area, old Cairo, Egypt. Ain Shams Eng. J. 3 (4), 349–358.
Helmi, F.M., Hefni, Y.K., 2016. Nanocomposites for the protection of granitic obelisks at Tanis, Egypt. Mediter. Archaeol. Archaeom. 87-96, 16(2).
Hendrickx, S., Claes, W. (2017). Bibliography of the Prehistory and the Early Dynastic Period of Egypt and Northern Sudan. 2017 Addition. Archéo-Nil, 27(1), 75–89.
Howland, M.D., Thompson, V.D., 2024. Modeling the potential impact of storm surge and sea level rise on coastal archaeological heritage: A case study from Georgia. PLoS One 19 (2), e0297178.
Hussain, M.S., Abd-Elhamid, H.F., Javadi, A.A., Sherif, M.M., 2019. Management of seawater intrusion in coastal aquifers: a review. Water 11 (12), 2467.
Hussien, R., Rayan, R., El-Aassar, A., 2021. Inverse geochemical modeling of groundwater salinization in El-tur South Sinai, Egypt. J. Basic Environ. Sci. 8, 16–28.
Ikuemonisan, F.E., Ozebo, V.C., Olatinsu, O.B., 2020. Geostatistical evaluation of spatial variability of land subsidence rates in Lagos, Nigeria. Geodesy Geodynam. 11 (5), 316–327.
Islam, M.S., 2023. Industrial water quality. In: Hydrogeochemical Evaluation and Groundwater Quality. Springer Nature Switzerland, Cham, pp. 281–299.
Jasechko, S., Perrone, D., Seybold, H., Fan, Y., Kirchner, J., 2020. Groundwater level observations in 250,000 coastal US wells reveal scope of potential seawater intrusion. Nature Communications 3229.
Kadam, A., Wagh, V., Patil, S., Umrikar, B., Sankhua, R., Jacobs, J., 2021. Seasonal variation in groundwater quality and beneficial use for drinking, irrigation, and industrial purposes from Deccan basaltic region, Western India. Environ. Sci. Pollut. Res. 28, 26082–26104.
Kaiser, M.F., El Rayes, A., Ghodeif, K., Geriesh, B., 2013. GIS data integration to manage waterlogging problem on the eastern nile delta of Egypt. Int. J. Geosci. 4 (4), 8.
Kalyani, D.S., Rajesh, V., Reddi, E.U., Kumar, K.C., Rao, S.S., 2017. Correlation between corrosion indices and corrosiveness of groundwater: a study with reference to selected areas of Krishna District, Andhra Pradesh, India. Environ. Earth Sci. 76, 1–13.
Kaur, G., Singh, G., Motavalli, P.P., Nelson, K.A., Orlowski, J.M., Golden, B.R., 2020. Impacts and management strategies for crop production in waterlogged or flooded soils: A review. Agron. J. 112 (3), 1475–1501.
Kumar, R., Kumari, A., Kumar, R., Sulaiman, M. A., Zafar, M. M., Singh, A., Prabhakar ,R Pippal, P. S.(2023). Assessing the geochemical processes controlling groundwater quality and their possible effect on human health in Patna, Bihar. Environ. Sci. Pollut. Res., 1–20.
Lecher, A.L., Watson, A., 2021. Danger from beneath: groundwater–sea-level interactions and implications for coastal archaeological sites in the southeast US. Southeast. Archaeol. 40 (1), 20–32.
Lian, H., Sun, Z., Xu, C., Gu, F., 2022. The relationship between the distribution of water and salt elements in arid irrigation areas and soil salination evolution. Front. Earth Sci. 10, 852485.
Lindsey, R., 2021. Climate change: Global sea level. Retrieved from vailable online: Climate. gov: https://www.climate.gov/news-features/understanding-climate/climate-changeglobal-sea-level (Accessed 20 March 2023).
Lu, C., Zhu, L., Li, X., Gong, H., Du, D., Wang, H., et al., 2022. Land subsidence evolution and simulation in the Western coastal area of Bohai Bay, China. J. Mar. Sci. Eng. 10 (10), 1549.
Lü, H., Zhu, J., Chen, Q., Li, M., Pan, S., Chen, S., 2023. Impact of estuarine reclamation projects on saltwater intrusion and freshwater resource. J. Oceanol. Limnol. 41 (1), 38–56.
Mabrouk, M., Jonoski, A., HP Oude Essink, G., Hlenbrook, S. (2018). Impacts of sea level rise and groundwater extraction scenarios on fresh groundwater resources in the Nile Delta governorates, Egypt. Water, 10(11), 1690.
Madani, A., Hagage, M., Elbeih, S.F., 2022. Random Forest and logistic regression algorithms for prediction of groundwater contamination using ammonia concentration. Arab. J. Geosci. 15 (20), 1619.
Mansour, B.M., 2012. Management of Groundwater Logging Problems along Wadi El-Tumilat, Eastern Nile Delta Using Mathematical Modeling and GIS Techniques. 220. M.Sc. thesis,. Fac. Science, Suez Canal Univ, Ismailia, Egypt.
Manunta, M., De Luca, C., Zinno, I., Casu, F., Manzo, M., Bonano, M., et al., 2019. The parallel SBAS approach for Sentinel-1 interferometric wide swath deformation time-series generation: algorithm description and products quality assessment. IEEE Trans. Geosci. Remote Sens. 57 (9), 6259–6281.
Masoud, M., El Osta, M., Alqarawy, A., Niyazi, B., 2023. Optimal management of the groundwater coastal aquifer based on the hydraulic characteristics in Wadi Al Marwani basin: KSA. Environ. Earth Sci. 82 (12), 308.
Megahed, H.A., 2020. GIS-based assessment of groundwater quality and suitability for drinking and irrigation purposes in the outlet and central parts of Wadi El-Assiuti, Assiut governorate, Egypt. Bull. Natl. Res. Cent. 44, 1–31.
Meister, J., Lange-Athinodorou, E., Ullmann, T., 2021. Preface: special issue "geoarchaeology of the Nile Delta". E&G Quat. Sci. J. 70 (2), 187–190.
Moorthy, P., Sundaramoorthy, S., Roy, P.D., Usha, T., Dash, S.K., Gowrappan, M., Chokkligam, L., 2024. Evaluation of spatial and temporal dynamics of seawater intrusion in coastal aquifers of Southeast India: insights from hydrochemical facies analysis. Environ. Monit. Assess. 196 (2), 1–14.
Mtibaa, S., Asano, S., 2022. Hydrological evaluation of radar and satellite gauge-merged precipitation datasets using the SWAT model: case of the Terauchi catchment in Japan. J. Hydrol. Region. Stud. 42, 101134.
Musa, Z., Popescu, I., Mynett, A., 2015. A review of applications of satellite SAR, optical, altimetry and DEM data for surface water modelling, mapping and parameter estimation. Hydrol. Earth Syst. Sci. 19, 3755–3769.
Nesterenko, P.N., 2023. Ion chromatography. In: Liquid Chromatography. Elsevier, pp. 465–507.
Orellana, F., Rivera, D., Montalva, G., Arumi, J.L., 2023. InSAR-based early warning monitoring framework to assess aquifer deterioration. Remote Sens. 15 (7), 1786.
Othman, A., Abdelmohsen, K., 2022. A geophysical and remote sensing-based approach for monitoring land subsidence in Saudi Arabia. In: Applications of Space Techniques on the Natural Hazards in the MENA Region. Springer International Publishing, Cham, pp. 477–494.
Ozegin, K.O., Ilugbo, S.O., Adebo, B., 2024. Spatial evaluation of groundwater vulnerability using the DRASTIC-L model with the analytic hierarchy process (AHP) and GIS approaches in Edo state, Nigeria. Phys. Chem. Earth Parts A/B/C 134, 103562.
Pennington, B.T., Sturt, F., Wilson, P., Rowland, J., Brown, A.G., 2017. The fluvial evolution of the Holocene Nile Delta. Quat. Sci. Rev. 170, 212–231.
Perumal, M., Sekar, S., Carvalho, P.C., 2024. Global investigations of seawater intrusion (SWI) in coastal Groundwaters in the last two decades (2000−2020): A bibliometric analysis. Sustainability 16 (3), 1266.
Prusty, P., Farooq, S., 2020. Seawater intrusion in the coastal aquifers of India-A review. HydroResearch 3, 61–74.
Puigserver, D., Giménez, J., Gràcia, F., Granell, À., Carmona, J.M., Torrandell, A., Fornós, J.J., 2024. Effects of global and climate change on the freshwater-seawater interface movement in a Mediterranean karst aquifer of Mallorca Island. Sci. Total Environ. 912, 169246.
Rachid, G., El-Fadel, M., Alameddine, I., AbouNajm, M., 2015. Vulnerability indices for SWI assessment. In: 35th Annual Conference of the International Association for Impact Assessment. Firenze Fiera Congress & Exhibition Center, Florence, Italy.
Ram, J., Dagar, J., Singh, G., Lal, K., Tanwar, V., Shoeran, S., ... & Kumar, M. (2008). Biodrainage: EcoFriendly Techniquefor Combating Waterlogging Salinity. Karnal: Central SoilSalinityResearchInstitute. 24pp.
Raspini, F., Caleca, F., Del Soldato, M., Festa, D., Confuorto, P., Bianchini, S., 2022. Review of satellite radar interferometry for subsidence analysis. Earth Sci. Rev. 104239.
Rateb, A., Abotalib, A.Z., 2020. Inferencing the land subsidence in the Nile Delta using Sentinel-1 satellites and GPS between 2015 and 2019. Sci. Total Environ. 729, 138868.
Reshi, A., Sandhu, H., Cherubini, C., Tripathi, A., 2023. Estimating land subsidence and gravimetric anomaly induced by aquifer overexploitation in the Chandigarh Tri-City region, India by coupling remote sensing with a deep learning neural network model. Water 15 (6), 1206.
Rezvi, H.U.A., Tahjib-Ul-Arif, M., Azim, M.A., et al., 2023. Rice and food security: climate change implications and the future prospects for nutritional security. Food Energy Sec. 12 (1), e430.
Rind, I.K., Khuhawar, M.Y., Jahangir, T.M., Memon, N., Lanjwani, M.F., Soomro, W.A., 2024. Water quality index and geographic information system to assess the groundwater quality of taluka Matiari, Sindh, Pakistan. Arab. J. Geosci. 17 (1), 15.
Sáenz-Martínez, Á., Pérez-Estébanez, M., San Andrés, M., de Buergo, M.A., Fort, R., 2021. Efficacy of acid treatments used in archaeological ceramics for the removal of calcareous deposits. Eur. Phys. J. Plus 136 (8), 798.
Saleh, M., Becker, M., 2019. New estimation of Nile Delta subsidence rates from InSAR and GPS analysis. Environ. Earth Sci. 78, 1–11.
Sangadi, P., Kuppan, C., Ravinathan, P., 2022. Effect of hydro-geochemical processes and saltwater intrusion on groundwater quality and irrigational suitability assessed by geo-statistical techniques in coastal region of eastern Andhra Pradesh, India. Mar. Pollut. Bull. 175, 113390.
Shah, M., Shah, V., Dudhat, K., Patel, D., 2023. Evaluation of geothermal water and assessment of corrosive and scaling potential of water samples in Tulsishyam geothermal region, Gujarat, India. Environ. Sci. Pollut. Res. 30 (15), 44684–44696.
Sidibe, A.M., Lin, X., Koné, S., 2019. Assessing groundwater mineralization process, quality, and isotopic recharge origin in the Sahel region in Africa. Water 11, 789.
Singh, A., 2024. Effective management of water resources problems in irrigated agriculture through simulation modeling. Water Resour. Manag. 38 (8), 2869–2887.

Singh, G., Lal, K., 2018. Review and case studies on biodrainage: An alternative drainage system to manage waterlogging and salinity. Irrigation and Drainage 67, 51–64.
Singh, R., Majumder, C.B., Vidyarthi, A.K., 2023. Assessing the impacts of industrial wastewater on the inland surface water quality: an application of analytic hierarchy process (AHP) model-based water quality index and GIS techniques. Phys. Chem. Earth Parts A/B/C 129, 103314.
Smith, B.J., Török, A., McAlister, J.J., Megarry, Y., 2003. Observations on the factors influencing stability of building stones following contour scaling: a case study of oolitic limestones from Budapest, Hungary. Build. Environ. 38 (9–10), 1173–1183.
Sojka, M., Kozłowski, M., Stasik, R., Napierała, M., Kęsicka, B., Wróżyński, R., Jaskuła, J., Liberacki, D., Bykowski, J., 2019. Sustainable water management in agriculture—the impact of drainage water management on groundwater table dynamics and subsurface outflow. Sustainability 11 (15), 4201.
Srinivasan, K., 2017. Ion Chromatography Instrumentation for Water Analysis. Chemistry and Water, pp. 329–351.
Stanley, J.D., Clemente, P.L., 2017. Increased land subsidence and sea-level rise are submerging Egypt's Nile Delta coastal margin. GSA Today 27 (5), 4–11.
Sutadian, A.D., Muttil, N., Yilmaz, A.G., Perera, B.J.C., 2017. Using the analytic hierarchy process to identify parameter weights for developing a water quality index. Ecol. Indic. 75, 220–233.
Taha, M.S., Armanuos, A.M., Zeidan, B.A., 2023. Impact of climate change on seawater intrusion, and shore line advance in Nile Delta, Egypt. Delta Univ. Sci. J 6 (2), 182–196.
Tomaszkiewicz, M., Abou Najm, M., El-Fadel, M., 2014. Development of a groundwater quality index for seawater intrusion in coastal aquifers. Environ. Model Softw. 57, 13–26.
Tran, D.D., Thuc, P.T.B., Park, E., Hang, P.T.T., Man, D.B., Wang, J., 2024. Extent of saltwater intrusion and freshwater exploitability in the coastal Vietnamese Mekong Delta assessed by gauging records and numerical simulations. J. Hydrol. 630, 130655.
Vallet, J.M., Hubert-Joly, E., Duberson, S., Leclère, F., 2022. Input of the technical imaging for the study of wall paintings: example of A lintel (tomb of KING TAKELOT I at TANIS san el-HAGAR, SHARQEYA, Egypt). Egypt. J. Archaeol. Restor. Stud. 12 (1), 73–87.
Vousdoukas, M.I., Clarke, J., Ranasinghe, R., et al., 2022. African heritage sites threatened as sea-level rise accelerates. Nat. Clim. Chang. 12, 256–262.
Yagoub, M.M., AlSumaiti, T., Tesfaldet, Y.T., AlArfati, K., Alraeesi, M., Alketbi, M.E., 2023. Integration of analytic hierarchy process (AHP) and remote sensing to assess threats to preservation of the oases: case of Al Ain, UAE. Land 12 (7), 1269.
Yu, Y., Zhi, J., Wei, B., Cheng, J., Hu, L., Lu, W., Gong, S., 2023. Seawater intrusion on the west coast of Shenzhen during 1980–2020 due to the influence of anthropogenic activities. Environ. Monit. Assess. 195 (5), 545.
Zaghloul, E. S. A, E. A. (2019). The geological evolution of some archaeological sites in the Nile Delta region,Egypt. In M. Baldi, G. C. Vittozzi, Sciences and Technologies Applied to Cultural Heritage I (STACH1) (p. 225). Roma: Cnr Edizioni.
Zhang, J.Z., Huang, H.J., Bi, H.B., 2015. Land subsidence in the modern Yellow River Delta based on InSAR time series analysis. Nat. Hazards 75, 2385–2397.